

Hysteresis Modeling and Experimental Verifications of Piezoelectric Ceramics Based Actuators

Mohammad Farhan Al Janaideh

A Thesis in the Department of Mechanical and Industrial Engineering

Presented in Partial Fulfillment of the Requirements for the

Degree of Master of Applied Science at

Concordia University

Montreal, Quebec, Canada

May 2004

© Mohammad F. Al Janaideh, 2004



Library and
Archives Canada

Bibliothèque et
Archives Canada

Published Heritage
Branch

Direction du
Patrimoine de l'édition

395 Wellington Street
Ottawa ON K1A 0N4
Canada

395, rue Wellington
Ottawa ON K1A 0N4
Canada

Your file *Votre référence*

ISBN: 0-612-94722-X

Our file *Notre référence*

ISBN: 0-612-94722-X

The author has granted a non-exclusive license allowing the Library and Archives Canada to reproduce, loan, distribute or sell copies of this thesis in microform, paper or electronic formats.

L'auteur a accordé une licence non exclusive permettant à la Bibliothèque et Archives Canada de reproduire, prêter, distribuer ou vendre des copies de cette thèse sous la forme de microfiche/film, de reproduction sur papier ou sur format électronique.

The author retains ownership of the copyright in this thesis. Neither the thesis nor substantial extracts from it may be printed or otherwise reproduced without the author's permission.

L'auteur conserve la propriété du droit d'auteur qui protège cette thèse. Ni la thèse ni des extraits substantiels de celle-ci ne doivent être imprimés ou autrement reproduits sans son autorisation.

In compliance with the Canadian Privacy Act some supporting forms may have been removed from this thesis.

Conformément à la loi canadienne sur la protection de la vie privée, quelques formulaires secondaires ont été enlevés de cette thèse.

While these forms may be included in the document page count, their removal does not represent any loss of content from the thesis.

Bien que ces formulaires aient inclus dans la pagination, il n'y aura aucun contenu manquant.

Canada

ABSTRACT

Hysteresis Modeling and Experimental Verifications of Piezoelectric Ceramics

Based Actuators

Mohammad Farhan Al Janaideh

There is an increasing usage of piezoceramic actuators in micropositioning applications, because they offer many desirable properties, such as fast response, high stiffness, and no backlash. Since piezoceramic materials are ferroelectric, they are fundamentally nonlinear in their response to an applied electric field, exhibiting a hysteresis effect between the electric field and the displacement. This usually causes undesirable inaccuracy or oscillations and even instability, which may severely limit the performance of the piezoceramic actuator system. One way to compensate hysteresis is to set up a model that adequately describes the hysteresis and use it in a control loop.

Focusing on a piezoelectric actuator from Physik Instrument Company, this thesis concentrates on modeling of hysteresis by using both the Preisach model and Prandtl-Ishlinskii model. The experiment on the hysteresis behavior of the piezoelectric actuator is carried out. Based on the measured data, a detailed discussion on the parameters identification for the two models is given and two models for the given piezoelectric actuator are therefore obtained. The validity of the two models is verified by comparing the actual and the model response of the piezoelectric actuator. The validity of the models is tested by comparing the actual and predicted response of the stacked piezoceramic actuator to input voltages.

DEDICATION

*I dedicate this work to my mother (Freidah Hassan) and my father (Farhan Ahmad) I ask
god to keep you for me*

ACKNOWLEDGMENTS

My modest thanks go to the great god, whom I submit my continuous gratitude, whenever I am alive and wherever I am dead.

I am very thankful to my respected supervisor Dr. C. Y. Su, for his enormous and unconditional support. I really appreciate His guidance, time, and effort. I would like to thank Dr. S. Rakheja for his help in arranging the experiment in CONCAVE. I would also like to thank the staffs of CONCAVE for helping me a lot while I was doing my experiment.

A great love and warm feelings submitted to my parents; to my mother, whom I need to spend hundreds of lives to award you; to my father, the source of my strength. Never ending thanks to, my handhold in the life, Fadi, Saeb, Bar'ha, Omar, Khaled, Ahmed, Yaman, and Hanan.

Finally, I gift this work to the residing in my heart, to whom concerned with my matter, to those tried to help even with a smile.

CONTENTS

List of Figures.....	viii
List of Tables.....	xiii
Nomenclature.....	xiv
Chapter 1 Introduction.....	1
1.1 Dynamic behavior.....	1
1.2 Benefits and Advantages.....	1
1.3 Applications of Piezoceramic Actuator.....	2
1.4 Hysteresis in Piezoceramic Actuator	3
1.5 Open and Closed-Loop Operations of the Piezoceramic Actuator.....	5
1.6 Scope of the Problem.....	6
1.7 Contribution of the Research.....	7
1.8 Research Objectives.....	7
1.8 Overview.....	9
Chapter 2: Mathematical Models of Hysteresis in Piezoceramic Actuators.....	10
2.1 Piezoceramic Actuator System.....	10
2.2 Review.....	12
2.3 Preisach model.....	13
2.3.1 Preisach Model description.....	14
2.3.2 Numerical Implementation.....	22
2.4 Prandtl-Ishlinskii Model.....	24
2.4.1 Play and Stop Operators.....	24

2.4.1.1 Stop Operator.....	25
2.4.1.2 Play Operator.....	26
2.4.2 Numerical Implementation.....	27
Chapter 3: Experimental Results.....	31
3.1 Experimental Setup.....	31
3.2 Experimental Results.....	36
Chapter 4: Hysteresis Modeling in Piezoceramic Actuator using Prandtl-Ishlinskii Model and Preisach model.....	40
4.1 Parameters Identification for Prandtl-Ishlinskii Model.....	40
4.2 Parameters Identification for Preisach Model.....	47
4.3 Comparison between Preisach model and Prandtl-Ishlinskii model.....	55
Chapter 5: Conclusion and Future work	56
References.....	58

LIST OF FIGURES

Chapter 1: Introduction.....	1
Figure 1.1: Hysteresis of piezoelectric material is rate-dependent. The plots show the response of a TS18-H5-104 (Piezo Systems, Inc.) piezoelectric actuator at two different driving frequencies.....	4
Figure 1.2 Measured piezoelectric stack actuator displacement response for 1 Hz exponential decreasing sinusoidal voltage input	4
Figure1.3: Measured hysteresis loop in piezoceramic actuator at 100 Hz sinusoidal voltage input.....	7
Chapter 2: Mathematical Models of Hysteresis in Piezoceramic Actuators.....	10
Figure2.1:Piezoceramics actuator system.....	10
Figure 2.2: $u(t)$ -Input voltage.....	11
Figure 2.3: $w(t)$ -Piezoceramic displacement	11
Figure 2.4: Hysteresis in piezoceramic actuator.....	12
Figure 2.5: Hysteresis operator.....	15
Figure 2.6: $\alpha - \beta$ diagram.....	15
Figure 2.7: $\alpha - \beta$ diagram.....	16
Figure 2.8: $\alpha - \beta$ diagram for initial state.....	17
Figure 2.9: Input voltage.....	17

Figure 2.10: $\alpha - \beta$ diagram for ascending input voltage.....	18
Figure 2.11: Input voltage.....	19
Figure 2.12: $\alpha - \beta$ diagram for descending input voltage.....	19
Figure 2.13: Input voltage.....	20
Figure 2.14: $\alpha - \beta$ diagram for ascending input voltage.....	20
Figure 2.15: $\alpha - \beta$ diagram for input voltage.....	21
Figure 2.16: $\alpha - \beta$ diagram for input voltage.....	22
Figure 2.17: Division of the voltage limiting triangle into a finite number of squares and triangle.....	23
Figure 2.18: Stop operator.....	25
Figure 2.19: Play operator.....	26
Figure 2.20: Physical model for the play operator.....	26
Figure 2.21: Stop operator.....	28
Figure 2.22 Piezoceramic actuator response at 0.1 Hz.....	29
Figure 2.23 Sinusoidal input voltage at 0.1 Hz.....	29
Figure 2.24: Prandtl-Ishlinskii model for sinusoidal input voltage at 0.1 Hz	30
Figure 2.25: Simulated hysteresis loop at 0.1 Hz.....	30
Chapter 3: Experimental Setup.....	31
Figure 3.1.a: Experimental setup.....	31

Figure 3.1.b: Experimental setup.....	32
Figure 3.2: Function generator 33210A.....	33
Figure 3.3: Piezo stack actuator & capacitive sensor P-753.31C.....	33
Figure 3.4: LVPZT amplifier module E-505.....	34
Figure 3.5: Microprocessor-controlled interface and display module E-516.....	34
Figure 3.6:E-515.C1, E-505,and E-516.....	35
Figure 3.7: Hysteresis loop.....	35
Figure 3.8: Hysteresis in piezoceramic actuator at different frequencies.....	38
 Chapter 4: Hysteresis Modeling in Piezoceramic Actuator using Prandtl-Ishlinskii Model and Preisach model.....	 39
Figure 4.1: Measured and predicted displacement in piezoceramic actuator at 0.10 Hz sinusoidal voltage input (Prandtl-Ishlinskii Model).....	40
Figure 4.2: Measured and predicted hysteresis loop in piezoceramic actuator at 0.10 Hz sinusoidal voltage input (Prandtl-Ishlinskii Model)	41
Figure 4.3: Predicted error of displacement in piezoceramic actuator at 0.10 Hz sinusoidal voltage input (Prandtl-Ishlinskii Model).....	41
Figure 4.4: Measured and predicted displacement in piezoceramic actuator at 10 Hz sinusoidal voltage input (Prandtl-Ishlinskii Model).....	42
Figure 4.5: Measured and predicted hysteresis loop in piezoceramic actuator at 10 Hz sinusoidal voltage input (Prandtl-Ishlinskii Model).....	43
Figure 4.6: Predicted error of displacement in piezoceramic actuator at 10 Hz sinusoidal voltage input (Prandtl-Ishlinskii Model).....	43

Figure 4.7: Measured and predicted hysteresis loop in piezoceramic actuator at 100 Hz sinusoidal voltage input (Prandtl-Ishlinskii Model).....	44
Figure 4.8: Measured and predicted hysteresis loop in piezoceramic actuator at 100 Hz sinusoidal voltage input (Prandtl-Ishlinskii Model).....	45
Figure 4.9: Predicted error of displacement in Piezoceramic actuator at 100 Hz sinusoidal voltage input (Prandtl-Ishlinskii Model).....	45
Figure 4.10: Measured and predicted displacement in piezoceramic actuator at 0.10 Hz sinusoidal voltage input (Preisach Model).....	47
Figure 4.11: Predicted hysteresis loop in piezoceramic actuator at 0.10 Hz sinusoidal voltage input (Preisach Model).....	48
Figure 4.12: Measured and predicted hysteresis loop in piezoceramic actuator at 0.10 Hz sinusoidal voltage input (Preisach Model).....	48
Figure 4.13: Predicted error of displacement in piezoceramic actuator at 0.10 Hz sinusoidal voltage input (Preisach Model).....	49
Figure 4.14: Measured and predicted displacement in piezoceramic actuator at 10 Hz sinusoidal voltage input (Preisach Model).....	49
Figure 4.15 Predicted error of displacement in piezoceramic actuator at 10 Hz sinusoidal voltage input (Preisach Model).....	51
Figure 4.15: Measured and Predicted hysteresis loop in piezoceramic actuator at 10 Hz sinusoidal voltage input (Preisach Model).....	51
Figure 4.16: Predicted error of displacement in piezoceramic actuator at 10 Hz sinusoidal voltage input (Preisach Model).....	51

Figure 4.17: Measured and predicted displacement in piezoceramic actuator at 100 Hz sinusoidal voltage input (Preisach Model).....	52
Figure 4.18: Measured and predicted hysteresis loop in piezoceramic actuator at 100 Hz sinusoidal voltage input (Preisach Model).....	53
Figure 4.19: Predicted error of displacement in piezoceramic actuator at 100 Hz sinusoidal voltage input (Preisach Model).....	54

LIST OF TABLES

Table 4.1: Nonlinearity in piezoceramic actuator at 70 sinusoidal voltages at different frequencies.....	37
Table 5.1: Identified parameters of the Prandtl-Ishlinskii model.....	41
Table 5.2: Error of predicted (Prandtl-Ishlinskii and Preisach) piezo response in piezo actuator at different frequencies.....	55

NOMENCLATURE

$\gamma_{\alpha\beta}[u](t)$	Preisach operator
$y(t)$	Piezocermics actuator displacement
α	“Up” switching values of the input voltage $u(t)$
β	“Down” switching values of the input voltage $u(t)$
$u(t)$	Input voltage
$v(t)$	Input voltage
$\mu(\alpha, \beta)$	Preisach function
$X(\alpha, \beta)$	Contraction of a piezo when the input increases and decreases
$E_r[v](t)$	Stop operator
$F_r[v](t)$	Play operator
r	Threshold
$p(r)$	Density function for Prandtl-Ishlinskii model
T	Limiting triangle
$W[.]$	Hysteric operator
$P[.]$	Prandtl operator

Chapter 1

Introduction

In 1880, Jacques and Pierre Curie discovered that pressure applied to a quartz crystal creates an electrical charge in the crystal [1]. They called this phenomenon the piezo effect. Later they also verified that an electrical field applied to the crystal would lead to a deflection of the material. This effect is referred to as the inverse Piezo effect. After the discovery, it took several decades to utilize the piezoelectric phenomenon.

1.1 Dynamic Behavior

Piezoactuator offers the fastest response time available (microsecond time constants). Acceleration rates of more than 10,000g can be obtained. Rise times on the order of microseconds and accelerations of more than 10,000g are possible [22]. This feature makes piezoceramic actuator suitable for rapid switching applications, precision positioning and micropositioning applications. Injector nozzle valves, hydraulic valves, electrical relays, adaptive optics and optical switches are a few examples of fast switching applications [1].

1.2 Benefits and Advantages

Piezoceramic actuators are increasingly used in high precision and high speed position control applications because of the following advantages [22, 1]:

- **Unlimited Resolution:** piezoelectric actuator can produce extremely fine position changes down to the sub-nanometer range. The smallest changes in operating voltage are converted into smooth movements.

- No magnetic fields: piezoelectric effect is related to electric fields. Piezoelectric actuators do not produce magnetic fields nor are they affected by them.
- Large force generation: piezoelectric can generate forces of several 10,000 N. Units move loads up to several tons of position over a range of more than 100 μm with sub-nanometer resolution.
- Rapid response: piezoactuator offers the fastest response time available (microsecond time constants). Acceleration rates of more than 10,000 g's can be obtained.
- Low Power Consumption: in a piezoelectric electrical energy is converted directly into motion, absorbing electrical energy during movement only. Static operation, even holding heavy loads, consumes virtually no energy.
- Complete absence of wear and tear: piezoceramic actuator displacement is based on solid-state phenomena and exhibits no wear and tear.

1.3 Applications of Piezoceramic Actuator

Piezoactuator became available around 20 years ago and have changed the world of precision positioning and micropositioning [1]. These applications include micromachining [2, 3, 22, 27], microrobotic applications [7], force control of a flexible robotic finger [4], positioning in hard disk drives [5], antenna shape control [6], micropump–fabrication of a micropump [7], precision turning of shafts on conventional CNC [8], and position tracking control of an optical pick-up device [9].

Main applications of piezoactuator in mechanical engineering are as follows [22, 1]:

Microelectronics:

- Wafer and mask positioning.
- Critical dimensions measurement.
- Inspection systems.
- Vibration cancellation.

Precision mechanics and mechanical engineering:

- Vibration cancellation.
- Structural deformation.
- Out-of-roundness grinding, drilling, turning.
- Tool adjustment.
- Wear correction.
- Needle valve actuation.
- Micro pumps.
- Linear drives.
- Piezo hammers.
- Knife edge control in extrusion tools.

1.4 Hysteresis in Piezoceramic Actuator

Because piezoceramic materials are ferroelectric [34], they are fundamentally nonlinear in their response to an input voltage, exhibiting a hysteresis effect between the displacement and the input voltage (Figure 1.1).

Without modeling hysteresis in the controller design, the hysteresis in piezoceramic actuator will act as a phase lag (Figure 1.2), which has the potential to cause undesirable accuracy or oscillations and even leading to instability.

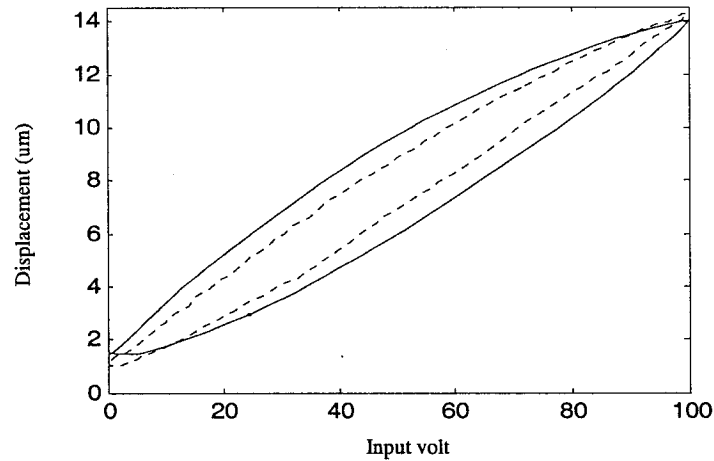


Figure 1.1: Hysteresis of piezoelectric material is rate-dependent. The plots show the response of a TS18-H5-104 (Piezo Systems, Inc.) piezoelectric actuator at two different driving frequencies [19].

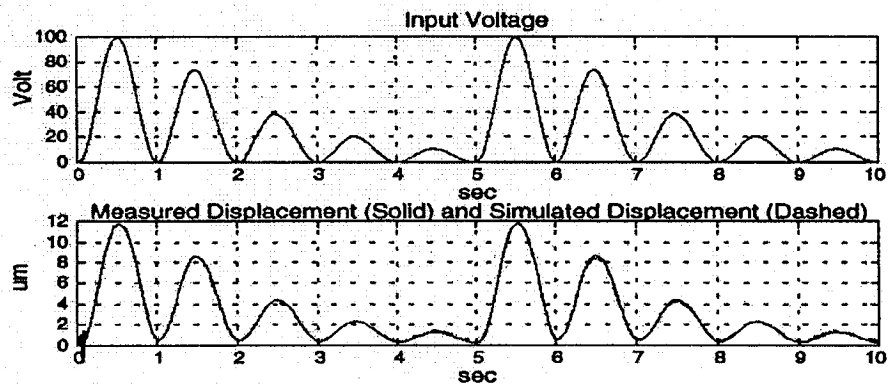


Figure 1.2: Measured piezoelectric stack actuator displacement response for 1 Hz exponential decreasing sinusoidal voltage input [20].

Ferroelectric are polycrystalline materials that contain many individually oriented ferroelectric grains and analogous to ferromagnetic materials within each grain there are clusters of aligned spontaneously electric dipoles called domains,

separated by imaginary domain walls [1, 15]. Initially, such ceramics are not piezoelectric even if the individual grains are; application of the small electric field will cause some electric dipoles to grow and others to shrink, so that there is no net change in strain. However, upon application of sufficiently large electric fields, some of the electric dipoles will switch directions, as a result, the domain walls will move, and there is now a net piezoelectric effect, this process is called poling. Hysteresis begins due to material defects and internal friction that can be considered as inertial forces that cause the dipoles to exhibit a preference for their current orientation [1, 15, 22].

Predication of hysteresis effect of piezoceramic actuator can facilitate the design of controllers to correct the disturbing of hysteresis. Moreover, a model based controller can be effectively realized to reduce the hysteresis effect.

1.5 Open and Closed-Loop Operation of the Piezoceramic Actuator

Piezoelectric actuators can be operated in open- and closed-loop modes. In open-loop mode, displacement roughly corresponds to the drive voltage. This mode is ideal when the absolute position accuracy is not critical, or when the position is controlled by data provided by an external sensor. Open-loop piezoceramic actuator exhibit hysteresis and creep behavior, just like other open-loop positioning systems. Closed-loop piezoceramic actuators are ideal for applications requiring high linearity, long-term position stability, repeatability and accuracy. Closed-loop piezoelectric actuators are equipped with position measuring systems providing sub-nanometer resolution or bandwidth up to 10 kHz [22].

1.6 Scope of the Problem

Because of the advantages of their nanometer displacement resolution, fast response, high stiffness, and no backlash, piezoceramic actuators have been used in micropositioning application. Piezoceramic materials are ferroelectric, they are fundamentally nonlinear in their response to an input voltage, exhibiting a hysteresis effect between the displacement and the input voltage (Figure 1.3). It was shown that the error at 800 Hz can be as large as 38.6% of the maximum piezo expansion [10].

Without modeling and incorporating hysteresis in the controller design, the hysteresis effect has the potential to cause undesirable accuracy or oscillations and even instability [32].

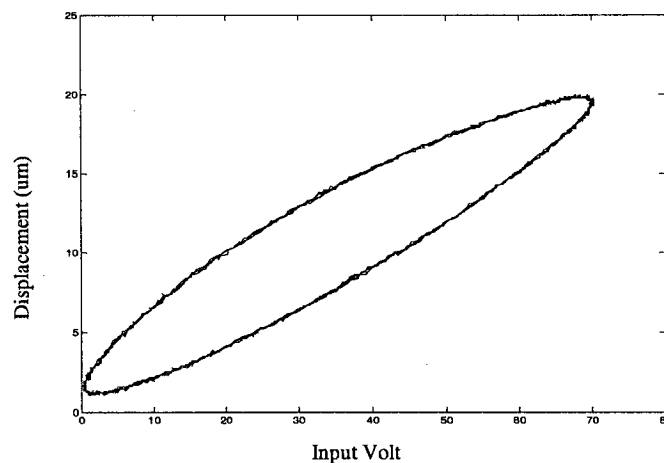


Figure 1.3: Measured hysteresis loop in piezoceramic actuator at 100 Hz sinusoidal voltage input.

During the last ten years there has been a steady growth in the study of various models for hysteresis in piezoelectric actuator. There are several hysteresis

models including those proposed by Preisach, Ishlinskii, Duhem, and karsanoel'skii-Pokrovskii [23].

1.7 Contribution of the Research

The principle contributions of this research are as follows;

- Parameter identification for the Prandtl-Ishlinskii model for characterizing the hysteresis in piezoceramic actuator.
- Development of a density function for a Prandtl-Ishlinskii model.
- Demonstrate that the hysteresis in piezoceramic actuator can be described smoothly, without complications in modeling.

We should mention that this work can be thought of as an initial step towards the controller design for removing the hysteresis effects, which will be pursued in the future during my PhD study.

1.7 Research objective

The goals of this research are three folds:

- (1) To describe the hysteresis behavior of piezoelectric actuators, by preferring perform the experiment on hysteresis behavior of a piezoactuator, and to compare the experimental measurements with the nominal input-output linear trajectory.

- (2) To test and explore the validity of the Prandtl-Ishlinskii model by comparing the predicted response of the stacked piezoceramic actuator to input voltages.
- (3) To perform a comparison between the Preisach model and Prandtl-Ishlinskii model.

In this thesis MATLAB 6.5, MATHEMATICA 4.0, and EXCEL are used in the numerical implementation. Nonlinear regression is used for Prandtl-Ishlinskii model using MATHEMATICA 4.0. Least square method in MATLAB and MATHEMATICA are used for Preisach model.

The particular objectives of this research can be summarized as follows:

- To describe the problems in piezoceramic actuator due to hysteresis;
- To briefly describe the mathematical models used to model hysteresis in piezoceramic actuator ;
- To identify the advantages and disadvantages of the Preisach model in hysteresis modeling in piezoelectric actuators;
- To estimate the advantages and disadvantages of the Prandtl-Ishlinskii in hysteresis modeling in piezoelectric actuators ;
- To describe the experimental setup and the experimental design to measure the displacement of the piezoelectric actuator;
- To describe the tools which are used to measure the signals and the displacement of the piezoactuator.

1.8 Overview

The thesis emphasized the hysteresis modeling in piezoceramic actuator through several chapters. In Chapter 2 two mathematical models were presented to generate hysteresis in piezoceramic actuators and complete reviews of previous research in this field are given. Also, numerical implementation and parameters identifications for the two models are presented. Chapter 3 describes the experimental setup and the experimental designs to measure the displacement of the piezoelectric actuator and describe the tools which are used to measure the signals and the displacement of the piezoactuator. In Chapter 4 the hysteresis and nonlinearity in piezoceramic actuator is brought under spotlight. Chapter 5 is modeling hysteresis using Preisach model and Prandtl-Ishlinskii model. Chapter 6 contains conclusion and future recommendations on this important topic.

Chapter 2

Mathematical Models of Hysteresis in Piezoceramic

Actuators

During the last ten years there has been a steady growth in the study of various models for hysteresis in piezoelectric actuator. There are several hysteresis models including those proposed by Preisach, Ishlinskii, Duhem, and karsanoel'skii-Pokrovskii [23]. The purpose of this chapter is to present mathematical models of hysteresis in piezoceramic.

2.1 Piezoceramic Actuator System

A block representation for the piezoceramic actuator is shown in Figure 2.1. The input $u(t)$ (Figure 2.2) is supplied to the piezoceramic actuator as a voltage. The piezoceramic actuator represented as W reacts to the input voltage by generating a displacement $w(t)$ (Figure 2.3). Hysteresis in piezoactuator is shown in Figure 2.4 which is a function of the input voltage and the output displacement.

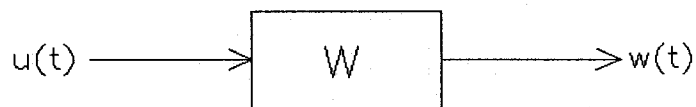


Figure 2.1: Piezoceramic actuator system

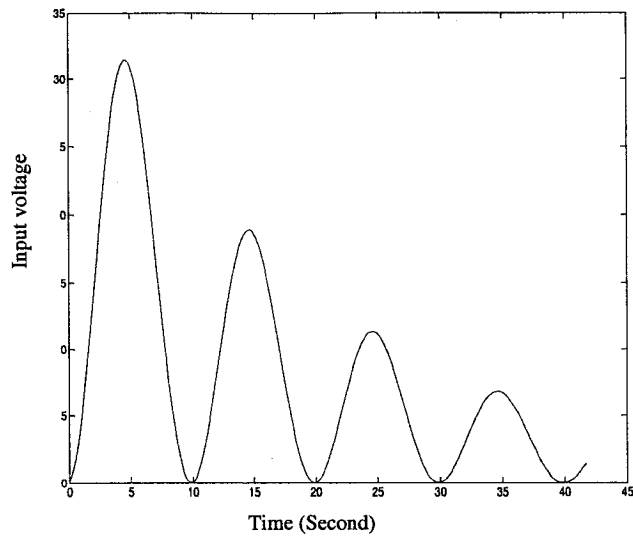


Figure 2.2: $u(t)$ - Input voltage

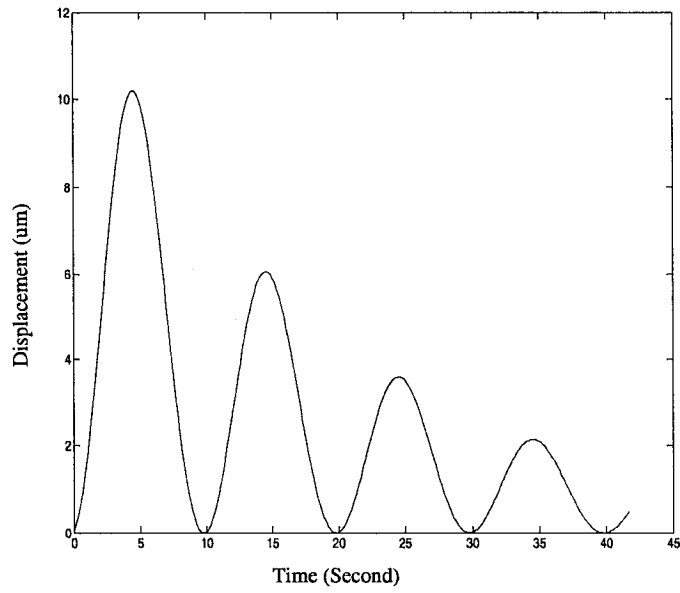


Figure 2.3: $w(t)$ - Piezoceramic displacement

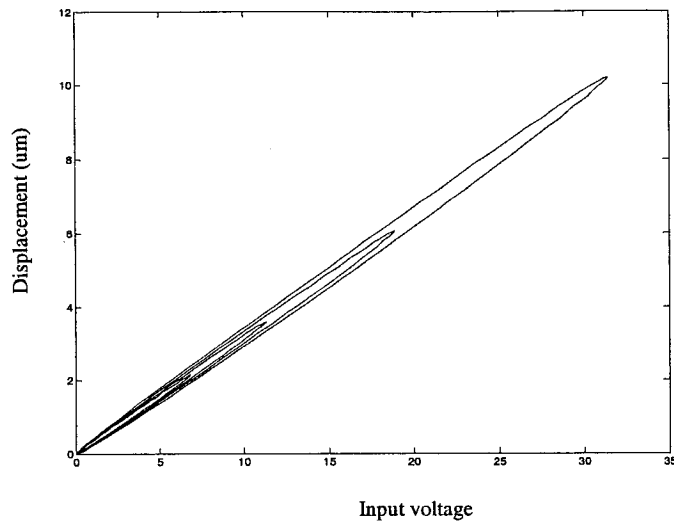


Figure 2.4: Hysteresis in piezoceramic actuator

Piezoelectric actuator is considered to have the property of scalar hysteresis if it exhibits the following properties for a single dimension of actuation [26]:

1. In Figure 2.4, the input voltage and output piezoceramic actuator response is bounded.
2. The input voltage and output piezoceramic actuator response is independent of the rate of the input.
3. On intervals, where input voltages are strictly increasing or strictly decreasing, the piezoceramic response also increase or decrease.

2.2 Review

Over the last ten years, there have been a number of mathematical models proposed for the hysteresis in piezoelectric actuator. Jung et al. [12] introduced deterministic hysteresis path models. These models can only describe the major loop of hysteresis. Ge and Joaneh [13, 14] generalized and adapted the Preisach model to describe the hysteresis in piezoelectric actuator; the accuracy was 3% within the working range of $(0-15)\mu m$. Hughes and Wen [15] discussed and verified the applicability of the classic Preisach model to piezoceramic material and shape memory alloys. The basic properties of the Preisach model were reviewed in [16, 28, 30]. Preisach model is capable of describing the input-output behavior of piezoceramic actuator. However, it is very difficult to construct its inverse function analytically [23], due to complexity of the Preisach model.

Stepanenko and Su adapted Duhem model to model hysteresis in piezoelectric actuator and used it in control [17]. Kuhlen and Janocha [18] used Prandtl-Ishlinskii operator to model the hysteresis in smart materials. Gallinaitis [26] used a Preisach type Karsanoel'skii-Pokrovskii (KP) operator to model and control piezoceramic actuator but Karsanoel'skii-Pokrovskii (KP) operator cannot accurately describe minor loops [21].

Choi, Lim and Choi used Maxwell slip model to control the hysteresis in piezoceramic actuator. Ang et al [19] developed a model to describe the rate dependent hysteresis in piezoceramic actuator by using Prandtl-Ishlinskii operator [19]. Tzan et al [20] described a novel method to describe hysteresis of piezoceramic actuator. Song and Li [21] extended the Preisach model using the

neural network to model rate dependent hysteresis in piezoceramic actuator. Adding neural networks to the modeling will complicate the mathematical model.

2.3 Preisach Model:

The Preisach model is one of the most widely used models that had been proposed by physicist Preisach in 1935 [24]. It has been used to model a variety of magnetic materials [25, 31]. The Preisach model of hysteresis has received considerable attention for many years, because it encompasses the basic feature of the hysteresis phenomena in theoretically simple and mathematically elegant way. Preisach model is capable of describing the input-output behavior of piezoceramic actuator with scalar hysteresis.

Classical Preisach model is developed for magnetic materials to describe the hysteresis [33, 31]. Nonlinearity of piezoceramic actuators differs from that of magnetic materials so there are modifications to use the Preisach model for piezoactuator [14, 13]. Ge and Joaneh [13,14] modified the Preisach model to describe the hysteresis in piezoelectric actuator . These modifications are:

- The Preisach operator $\gamma_{\alpha\beta}[u](t)$, which is used in the model, should be modified to either 0 or +1 instead of -1 or +1,since the piezoceramic actuator consists of polarized ceramic materials , which is applied in the direction of the polarization.
- A fixed piezoceramic polarization is produced because of the mechanical bias (the preload applied to piezoceramic actuators).

2.3.1 Preisach Model Description

The piezoceramic expansion response $y(t)$ to the excitation voltage $u(t)$ can be written as [11]:

$$y(t) = W[u](t) = \iint_{\alpha \geq \beta} \mu(\alpha, \beta) \gamma_{\alpha\beta}[u(t)](t) d\alpha d\beta \quad (2.1)$$

where $y(t)$ is the piezoceramic expansion, $u(t)$ is the input voltage, $\mu(\alpha, \beta)$ is Preisach function and $\gamma_{\alpha\beta}[\cdot]$ (Figure 2.5) is the hysteresis operator having the output +1 or 0 with switching values α and β that correspond to “up” and “down”. Geometrically this switching to the ‘up’ position leads to subdivision of the limiting triangle T into two areas which are S^+ and S^o (Figure 2.6).

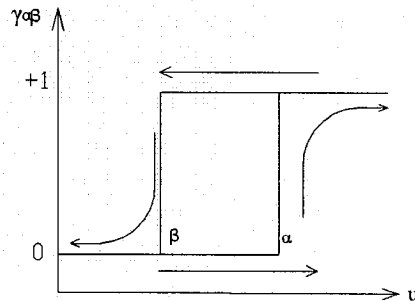


Figure 2.5: Hysteresis operator

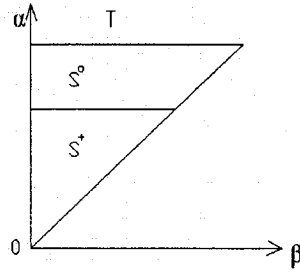


Figure 2.6: $\alpha - \beta$ diagram

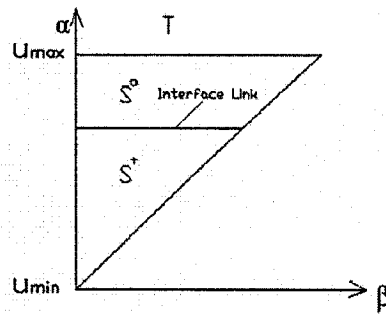


Figure 2.7: $\alpha - \beta$ diagram

Each operator can be represented by rectangular loop on the input voltage $u(t)$. The function $\mu(\alpha, \beta)$ is a weighting function and is called the Preisach function. The product of the Preisach function $\mu(\alpha, \beta)$ and the operator is integrated over the triangle T (2.2), which corresponds to $u_{max} \geq \alpha \geq \beta \geq u_{min}$, as shown in Figure 2.7.

$$y(t) = \iint_{S^+} \mu(\alpha, \beta) \gamma_{\alpha\beta}[u(t)](t) d\alpha d\beta - \iint_{S^0} \mu(\alpha, \beta) \gamma_{\alpha\beta}[u(t)](t) d\alpha d\beta \quad (2.2)$$

The regions $S^+(t)$ and $S^0(t)$ represent the hysteresis operator that is down and up, respectively. The interface $S(t)$ (Figure 2.7) is a staircase line which is

determined by the previous reversal input voltage. Since $\gamma_{\alpha\beta} = 1$, if $(\alpha, \beta) \in S^+$ and $\gamma_{\alpha\beta} = 0$, if $(\alpha, \beta) \in S^o$, the piezoceramic actuator expansion based on modified Preisach model is shown in 2.3:

$$y(t) = \iint_{S^+} \mu(\alpha, \beta) \gamma_{\alpha\beta}[u(t)](t) d\alpha d\beta \quad (2.3)$$

Assume that the input $u(t)$ at time t_o is 0 and all the hysteresis operator are at the down position (Figure 2.8). So, there is no expansion in piezoceramic actuator.

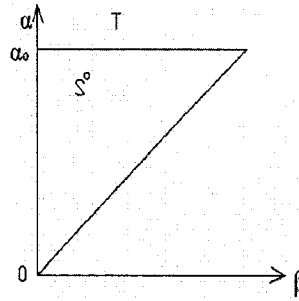


Figure 2.8: $\alpha - \beta$ diagram for initial state

As the input voltage increases from 0 to u_1 (Figure 2.9), all the hysteresis operators, whose up switching α value is less than the input u_1 , are turned to 'up' position (Figure 2.10) and the piezoceramic expansion is described as:

$$y(t) = \iint_{S^+} \mu(\alpha, \beta) \gamma_{\alpha\beta}[u(t)](t) d\alpha d\beta \quad (2.5)$$

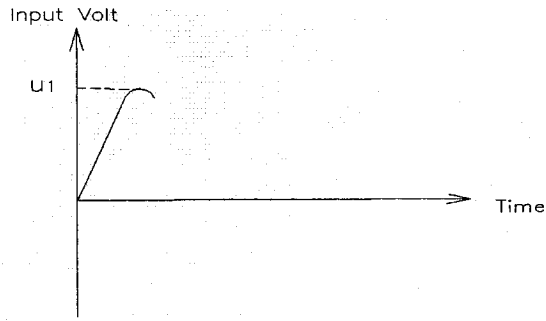


Figure 2.9: Input voltage

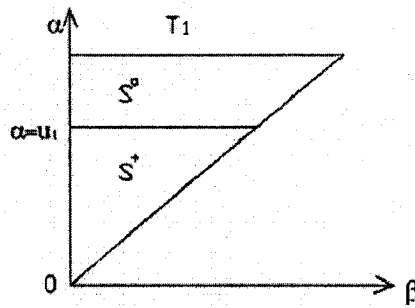


Figure 2.10: $\alpha - \beta$ diagram for ascending input voltage

When the input is decreased from u_1 to u_2 (Figure 2.11) all the hysteresis operators with down switching β larger than the current input voltage u_2 are turned to the 'down' position and thus will reduce S^+ area (Figure 2.12). As the result the piezoceramic expansion will be:

$$y(t) = \iint_{S^+} \mu(\alpha, \beta) \gamma_{\alpha\beta}[u(t)](t) d\alpha d\beta \quad (2.6)$$

In (2.7), $X(\alpha, \beta)$ is the amount of contraction of the piezoceramic when the input increases from 0 to u_1 and then decreases to u_2 .

$$X(\alpha, \beta) = x_\beta - x_{\alpha\beta} \quad (2.7)$$

where

$$x_\beta = \iint_{T_1} \mu(\alpha, \beta) \gamma_{\alpha\beta}[u(t)](t) d\alpha d\beta \quad (2.8)$$

and

$$x_{\alpha\beta} = \iint_{T_2} \mu(\alpha, \beta) \gamma_{\alpha\beta}[u(t)](t) d\alpha d\beta \quad (2.9)$$

where x_β (2.8) is the expansion form 0 to u_1 , and the second term $x_{\alpha\beta}$ (2.9) comes from decreasing the input voltage from u_1 to u_2 .

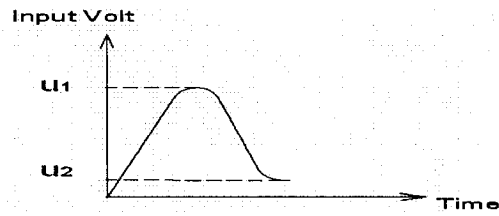


Figure 2.11: Input voltage

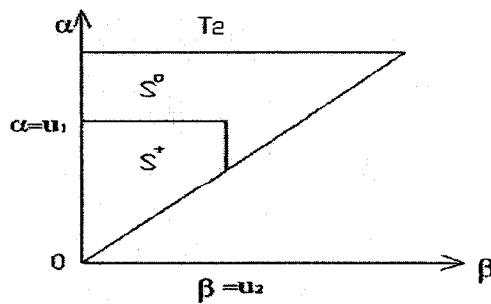


Figure 2.12: $\alpha - \beta$ diagram for descending input voltage

When the input increases again and reached u_3 (Figure 2.13), a new horizontal segment of the interface link will be created (Figure 2.14).

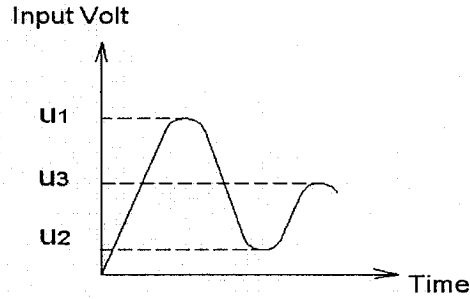


Figure 2.13: Input voltage

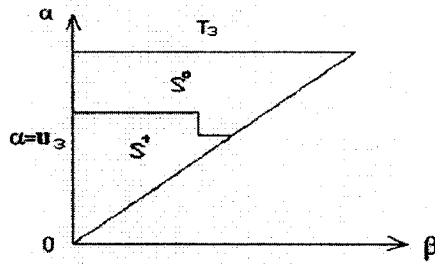


Figure 2.14: $\alpha - \beta$ diagram for ascending input voltage

The piezoceramic actuator response $y(t)$ based on Preisach plane (Figure 2.15)

when $\dot{u}(t) > 0$ is described in (2.16):

$$y(t) = \iint_{s^+} \mu(\alpha, \beta) d\alpha d\beta = \iint_{s_1^+} \mu(\alpha, \beta) d\alpha d\beta + \iint_{s_2^+} \mu(\alpha, \beta) d\alpha d\beta + \iint_{s_3^+} \mu(\alpha, \beta) d\alpha d\beta \quad (2.16)$$

then

$$y(t) = [X(\alpha_1, \beta_0) - X(\alpha_1, \beta_1)] + [X(\alpha_2, \beta_1) - X(\alpha_2, \beta_2)] + [X(u(t), \beta_2)] \quad (2.17)$$

So in general

$$y(t) = \sum_{k=1}^{n-1} [X(\alpha_k, \beta_{k-1}) - X(\alpha_k, \beta_k)] + X(u(t), \beta_{n-1}) \quad (2.18)$$

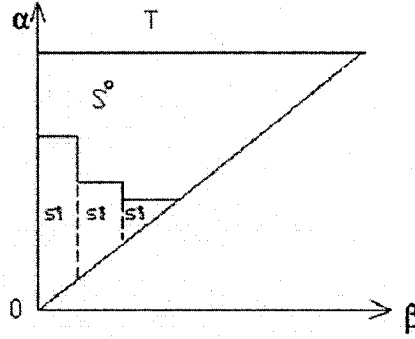


Figure 2.15: $\alpha - \beta$ diagram for input voltage

The piezoceramic actuator response $y(t)$ based on Preisach plane (Figure 2.16)

when $\dot{u}(t) < 0$ is described in (2.20) [13, 14]:

$$y(t) = \iint_{s^*} \mu(\alpha, \beta) d\alpha d\beta = \iint_{s_1^*} \mu(\alpha, \beta) d\alpha d\beta + \iint_{s_2^*} \mu(\alpha, \beta) d\alpha d\beta + \iint_{s_3^*} \mu(\alpha, \beta) d\alpha d\beta \quad (2.20)$$

then

$$y(t) = [X(\alpha_1, \beta_0) - X(\alpha_1, \beta_1)] + [X(\alpha_2, \beta_1) - X(\alpha_2, \beta_2)] + [X(u(t), u(t))] \quad (2.21)$$

So in general

$$y(t) = \sum_{k=1}^{n-1} [X(\alpha_k, \beta_{k-1}) - X(\alpha_k, \beta_k)] + [X(\alpha_n, \beta_{n-1}) - X(\alpha_n, u(t))] \quad (2.22)$$

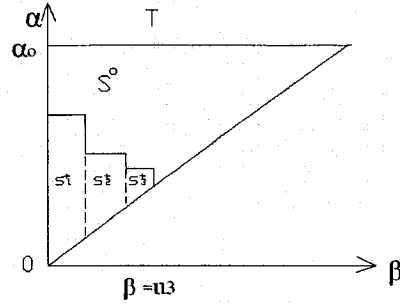


Figure 2.16: $\alpha - \beta$ diagram for input voltage

Preisach model is completely characterized by two properties [31]:

(1) Wiping-out property: The wiping out property refers to the constraint output that the output be affected only by the current input and the alternating series of pervious domain input exterma, the effect of all other inputs being wiped out.

(2) Congruent minor-loop property: The congruent minor-loop property requires that all equivalent minor loops be congruent. Two minor loops are said to be equivalent if they are generated by an input varying monotonically between the same two exterma.

2.3.2 Numerical Implementation

In (2.23) and (2.24) a numerical form of the Preisach model that can be formed to calculate the piezoelectric displacement [31].

$$\dot{u}(t) < 0, x(t) = \sum_{k=1}^{n-1} [X(\alpha_k, \beta_{k-1}) - X(\alpha_k, \beta_k)] + [X(\alpha_n, \beta_{n-1}) - X(\alpha_n, u(t))] \quad (2.23)$$

$$\dot{u}(t) > 0, x(t) = \sum_{k=1}^{n-1} [X(\alpha_k, \beta_{k-1}) - X(\alpha_k, \beta_k)] + X(u(t), \beta_{n-1}) \quad (2.24)$$

The numerical implementation procedure for the Preisach model to describe hysteresis in piezoceramic actuator was described in [31]. The procedure is:

- The input voltages history and the current input voltage are specified.
- Particular square cells for $\dot{u}(t) < 0$ or triangle cells $\dot{u}(t) > 0$ for the input voltages are determined (Figure 2.17).
- The Preisach function when $\alpha = \beta$ is:

$$f_{\beta} = a_0 + a_1 \cdot \alpha + a_2 \cdot \beta \quad (2.25)$$

and the Preisach function when $\alpha \neq \beta$ is:

$$f_{\alpha\beta} = b_0 + b_1 \cdot \alpha + b_2 \cdot \beta + b_3 \cdot \alpha \cdot \beta \quad (2.26)$$

The constants in the two equations are estimated on the measured displacement at the squares and triangles as shown in Figure 2.17.

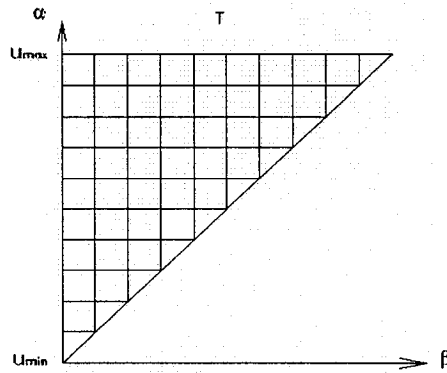


Figure 2.17: Division of the voltage limiting triangle into a finite number of squares and triangles.

Preisach model is capable of describing the input-output behavior of piezoceramic actuator. However, it is very difficult to construct its inverse function analytically [23], due to complexity of the Preisach model.

2.4 Prandtl-Ishlinskii Model

In 1928 L. Prandtl proposed to model the elastic-plastic behavior using the relation [40] in (2.27),

$$w(t) = \int_0^R p(r)E_r[v](t)dr, \quad (2.27)$$

where $p(r)$ is a density function and $E_r[v](t)$ is elastic-plastic element. In (2.27), the input-output relation $w(t)$ is obtained from the strain v through a weighted superposition of basic elastic-plastic elements. The operator defined in (2.28) is called Prandtl operator, and the denotation is

$$w = P[v], \quad (2.28)$$

this operator is referred to Ishlinskii operator [23].

Prandtl-Ishlinskii model is based on the play and stop hysteresis operators. This model has some very unique properties that are invertible and inversion has the same structure and satisfies the wipe-out property [37]. The stop and play operator are rate independent and Prandtl-Ishlinskii model is also rate independent.

2.4.1 Play and Stop Operators

One of the basic hysteresis nonlinearity is given by the stress-strain relation in a one-dimensional elastic plastic element, which is shown in Figure 2.18. As long as the modulus of the stress w is smaller than the yield stress r , the strain behavior v is related to w through the hook's law. Once the stress has reached the yield value, it remains constant under a further increase of the strain; however, the elastic behavior is instantly recovered when the strain is lowered again.

2.4.1.1 Stop Operator

The input-output relation can be expressed by an elastic-plastic, or stop operator (Figure 2.18), $w(t) = E_r[v](t)$, with the threshold r . Analytically, suppose $C_m[0, t_E]$ is the space of piecewise monotone continuous functions for any input $w(t) = E_r[v](t)$ is the space of piecewise monotone continuous functions, for any input $v(t) \in C_m[0, t_E]$,

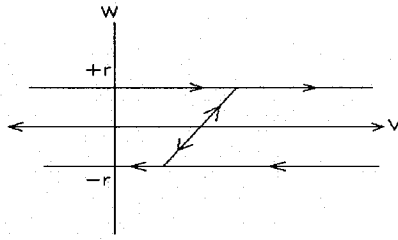


Figure 2.18: Stop operator

The stop operator, E_r , for any $r \geq 0$, can be given by the definition

$$E_r[v](0) = e_r(v(0)) \quad (2.29)$$

$$E_r[v](t) = e_r(v(t) - v(t_i) + E_r[v](t_i)) \quad (2.30)$$

for $t_i < t \leq t_{i+1}$ and $0 \leq i \leq N - 1$.

with
$$e_r(v) = \min(r, \max(-r, v)) \quad (2.31)$$

where $0 = t_0 < t_1 < \dots < t_N = t_E$ is a partition of $[0, t_E]$ such that the function v is monotone on each of the sub-intervals $[t_i, t_{i+1}]$, the argument of the operator is written in square brackets to indicate the functional dependence, since it maps a function to a function. The stop operator however is mainly characterized by its

threshold parameter r which determines the height of the hysteresis in the region $w - v$ plane.

2.4.1.2 Play Operator

Play operator is another basic hysteresis nonlinearity operator. The one-dimensional play operator (Figure 2.19) can be considered as a piston with plunger of length $2r$ (Figure 2.20). The output $w(t)$ is the position of the center of the piston, and the input is the plunger position $v(t)$. The input-output is given in (2.21).

$$F_r[v](0) = f_r(v(0), 0) \quad (2.32)$$

$$F_r[v](t) = f_r(v(t), f_r[v](t_i)), \text{ For } t_i < t \leq t_{i+1} \text{ and } 0 \leq i \leq N - 1,$$

with

$$f_r(v, w) = \max(v - r, \min(v + r, w)) \quad (2.33)$$

where $0 = t_0 < t_1 < \dots < t_N = t_E$ is a partition of $[0, t_E]$ such that the function v is monotone on each of the sub-intervals $[t_i, t_{i+1}]$.

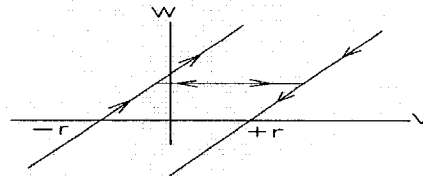


Figure 2.19: Play operator

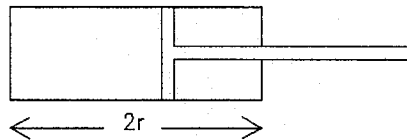


Figure 2.20: Physical model for the play operator

From the definitions in (2.20) and (2.22), it was proved [37] that the operator $F_r[v]$ is the complement of the $E_r[v]$, they are related through the equation

$$F_r[v](t) + E_r[v](t) = v(t) \quad (2.34)$$

for any piecewise monotone input function v and $r \geq 0$.

2.4.3 Numerical Implementation.

The piezoceramic actuator response based on Prandtl-ishlinskii model is:

$$y(t) = \int_0^R p(r)E_r[v](t)dr \quad (2.36)$$

$p(r)$ is a density function used in [36]:

$$p(r) = \alpha e^{-\beta(r-\delta)^2} \quad (2.37)$$

Because $E_r[v](t)$ is continuous function then:

$$y(t) = \int_0^r p(r)E_r[v](t)dr \quad (2.38)$$

so

$$y(t) = \sum_0^R p(r)E_r[v](t)(r_i - r_{i-1}) \quad (2.39)$$

then

$$y(t) = \sum_0^R (p(r)E_r[v](t)r_i - p(r)E_r[v](t)r_{i-1}) \quad (2.40)$$

$$y(i) = \sum_0^R (y(i) - y(i-1)) \quad (2.41)$$

Example:

If we have a piezoceramic actuator which subjected to a sinusoidal input voltage of the form (Figure 2.22):

$$v(t) = (20 + 20 \sin(0.2\pi t + \phi))e^{-0.051t} \quad (2.42)$$

and the stop operator is $E_r[v](t)$ (Figure 2.21) and r is:

$$r = 0.133 + 0.40517v \quad (2.43)$$

with density function $p(r)$ (Figure 2.24) is:

$$p(r) = 6.5.e^{-0.00305(r-4)^2} \quad (2.44)$$

then, modeling the response of the piezoceramic actuator (Figure 2.23) using the Prandtl-Ishlinskii model (Figure 2.24) is :

$$y(t) = \sum_0^R (p(r)E_r[v](t)r_i - p(r)E_r[v](t)r_{i-1}) \quad (2.45)$$

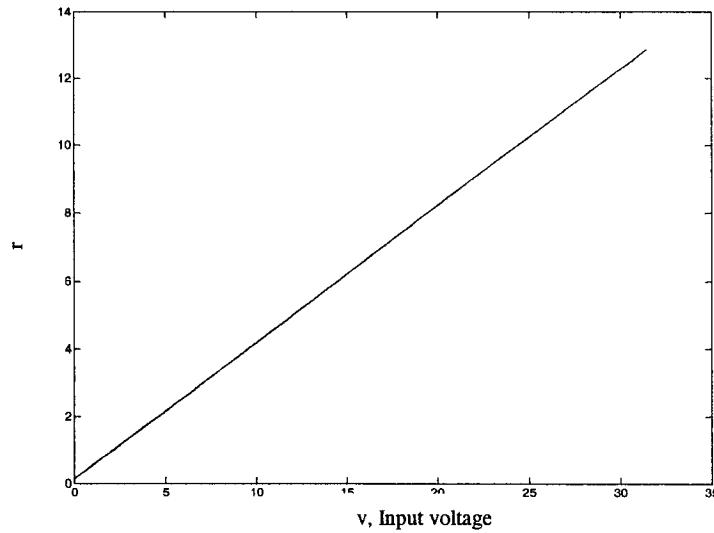


Figure 2.21 Stop operator

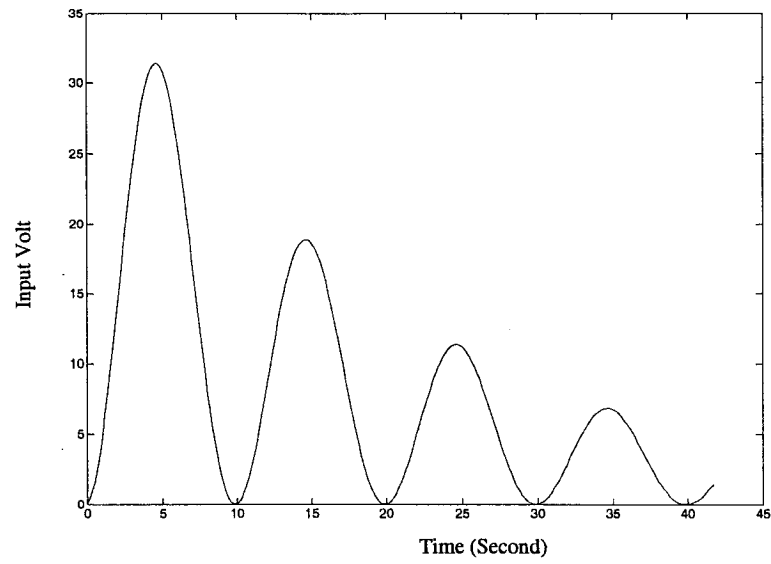


Figure 2.22 Sinusoidal input voltage at 0.1 Hz

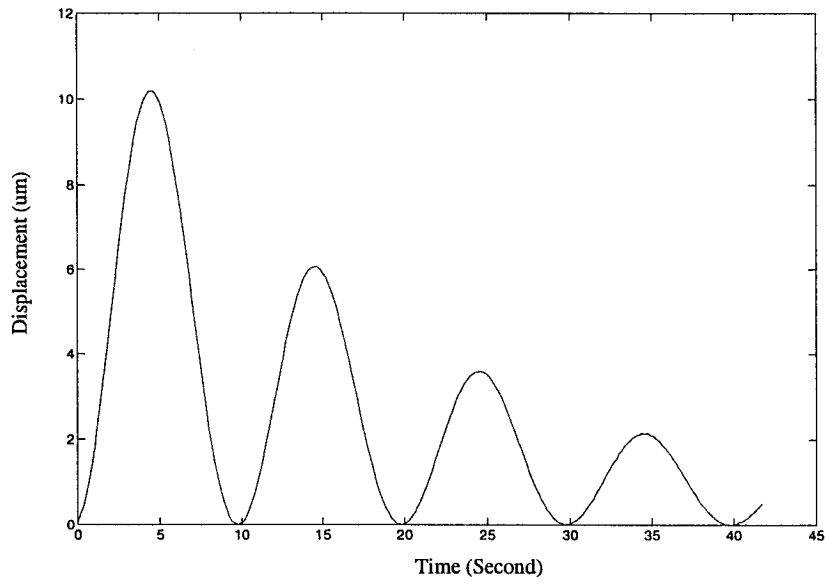


Figure 2.23 Piezoceramic actuator displacement 0.1 Hz

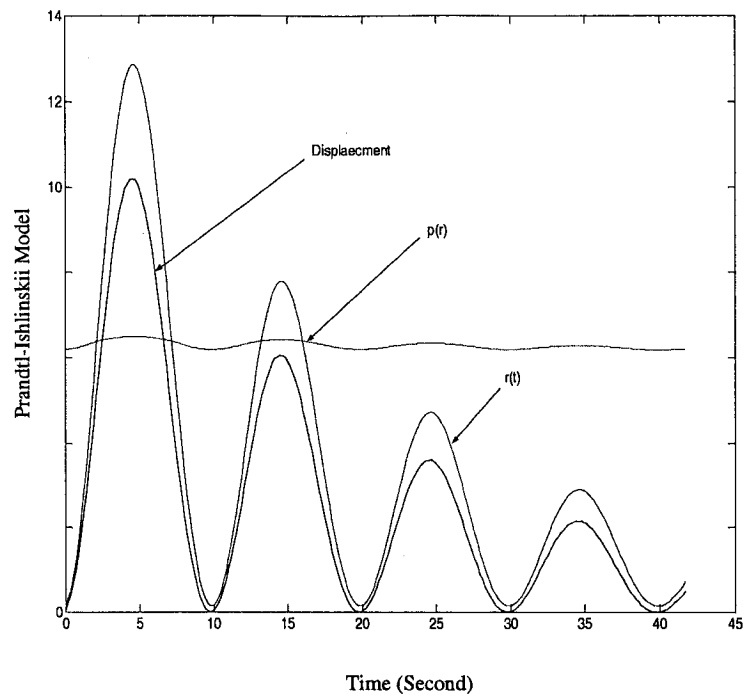


Figure 2.24: Prandtl-Ishlinskii model

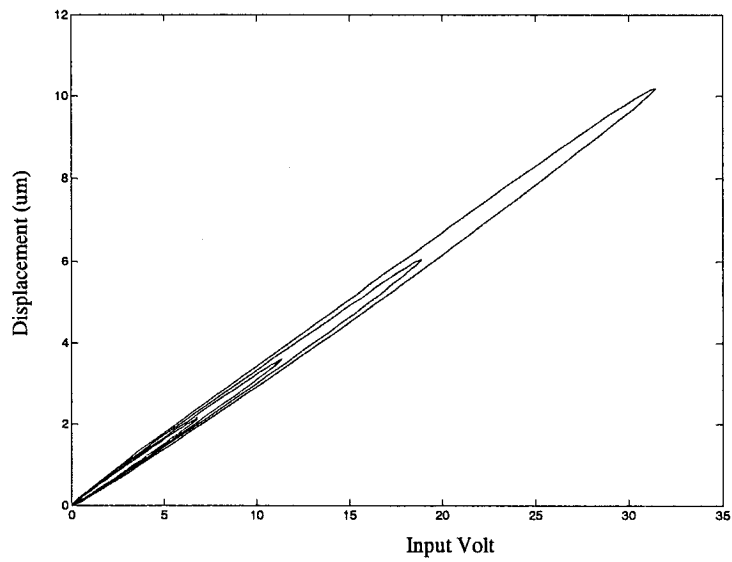


Figure 2.25: Simulated hysteresis loop at 0.1 Hz

Chapter 3

Experimental Results

3.1 Experimental Setup:

The experimental set up that is shown in Figures 3.1.a and 3.1.b is used to record the input voltage and the displacement response of an unloaded piezoceramic actuator made by PI (Physik Instrumente) company. Piezo stack actuator (P-753.31C) used in experiment is extremely fast and compact device, providing a positioning and scanning range of up to $22\ \mu\text{m}$ with very fast settling .

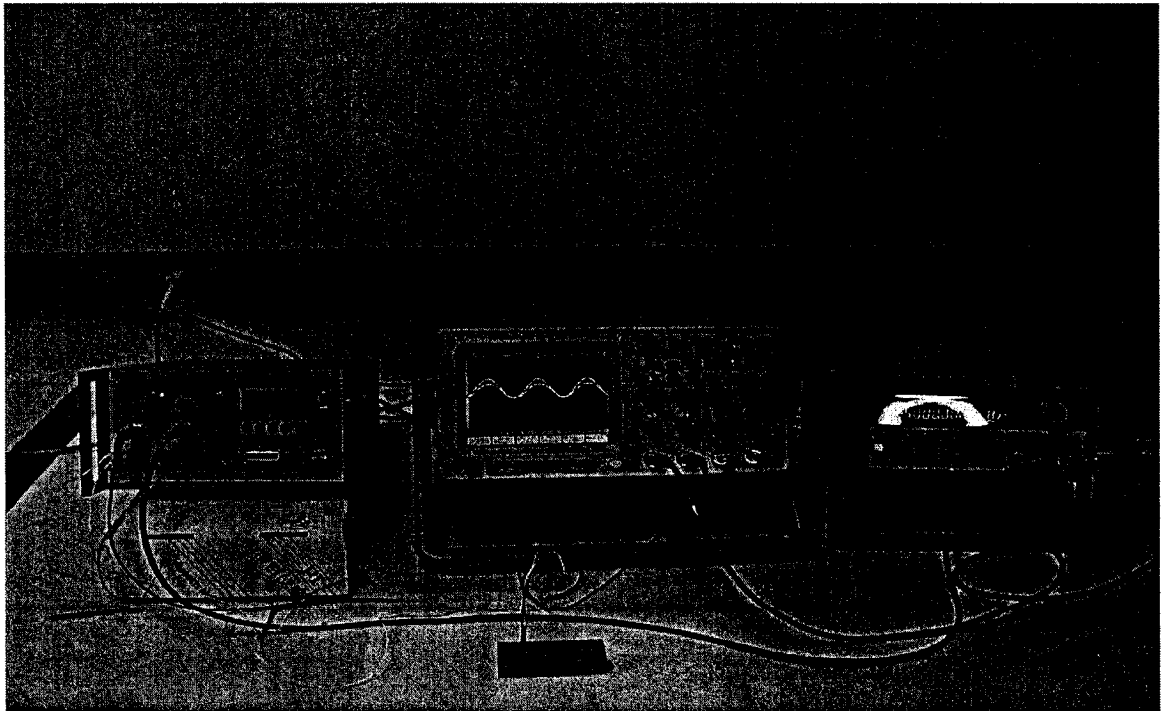


Figure 3.1.a: Experimental setup

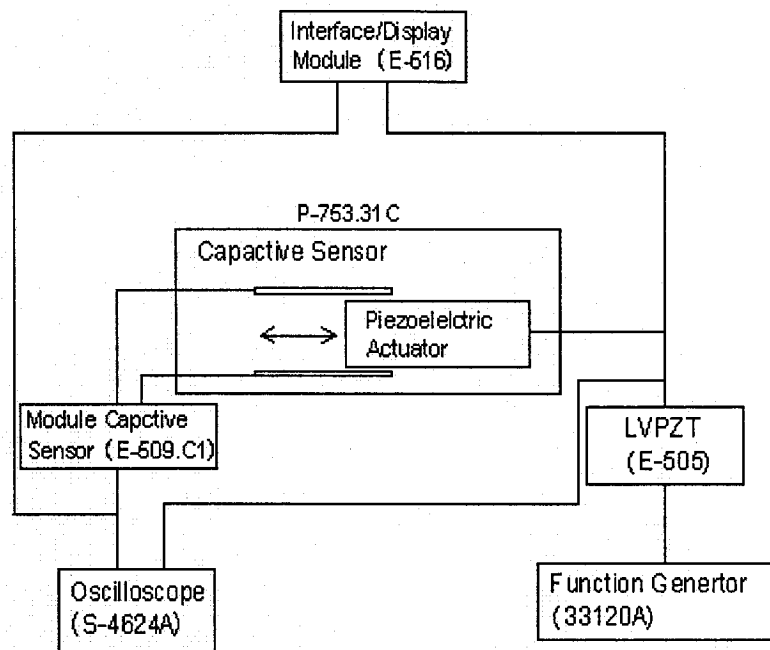


Figure 3.1.b: Experimental set up

Piezoceramic actuator (Model P-753.31C from Physik Instrumente company) (Figure 3.3) has nominal displacement of 0-38 μm for input voltages of 0 to 100 V. A function generator (33210A) (Figure 3.2) was used to produce positive voltages with amplitudes in the range 0 to +7 and 0 to +4 volts at different frequencies. LVPZT (E-505) (Figure 3.4) - amplifier module (single channel amplifier for low voltages piezoceramic) with average current of 300 mA was used to operate the piezo in the range from 0 to 100 volts. Output voltages can be controlled by the 10-turn manual potentiometers located at the front panel. DC offset potentiometer is active at the same time. Internally it produces an offset voltage from 0 to 10 volts to the input signal.



Figure 3.2: Function Generator (33210A)

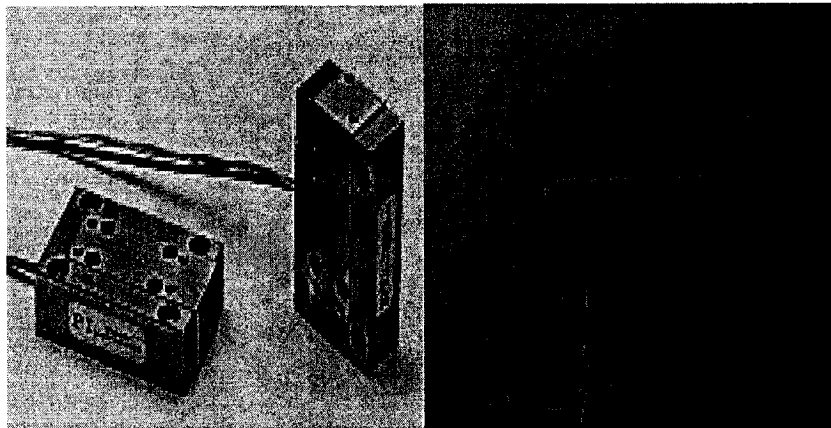


Figure 3.3: Piezo stack actuator and capacitive sensor (P-753.31C)

A capacitive sensor was used to measure the displacement of the stack resulting from the varying input. The capacitive sensor provide excellent resolution (better than 0.1 nm), long-term and temperature stability. The capacitance of plate capacitor depends on the distance between both plates called probe and target.

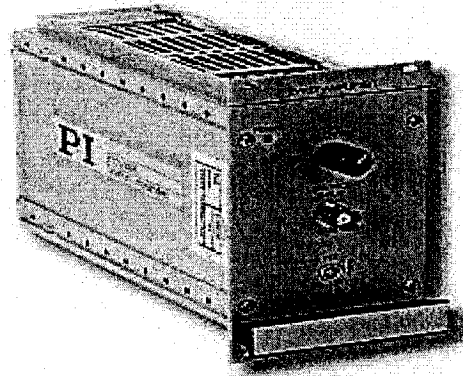


Figure 3.4: LVPZT amplifier module E-505

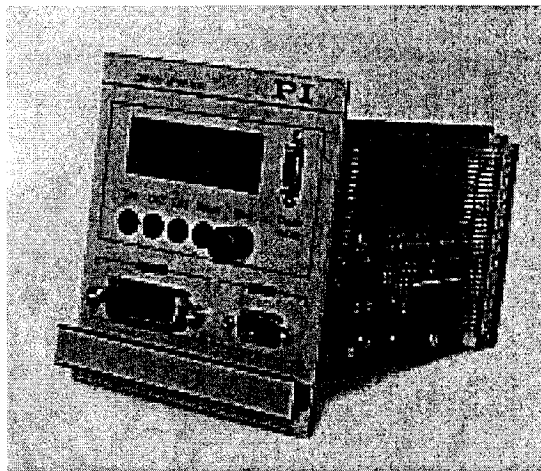


Figure 3.5: Microprocessor-controlled interface and display module (E-516)

A microprocessor-controlled interface and display module with integrated 20-bit D/A converters is shown in Figures 3.5 and 3.6 . Figure 3.7 shows experimental voltage-to-displacement curve in piezoceramic actuator at 100 Hz sinusoidal input voltage.

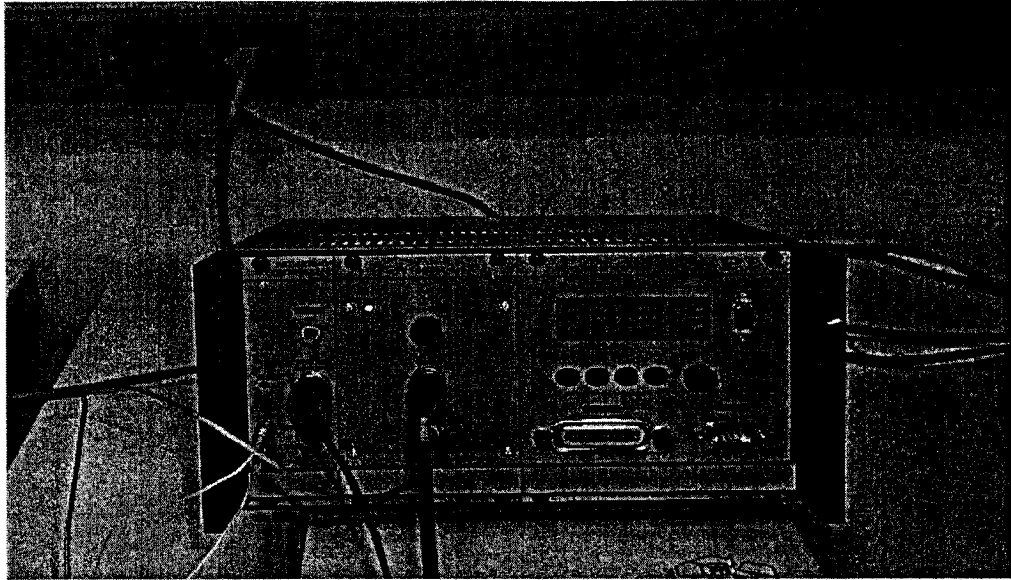


Figure 3.6: (from left to right-Capacitive Module E-515.C1, LVPZT Amplifier Module E-505, Microprocessor-Controlled Interface and Display Module E-516)

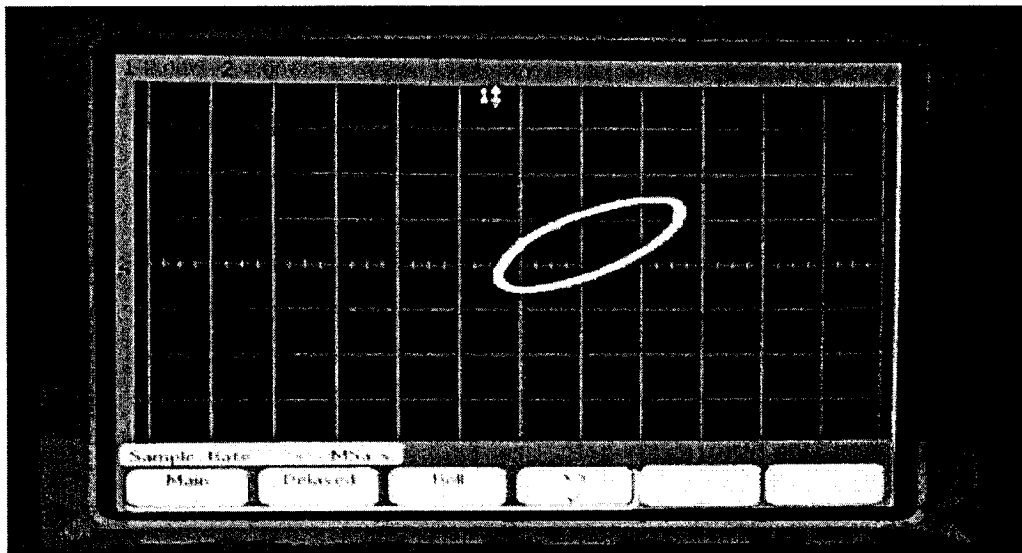


Figure 3.7: Hysteresis loop

3.2 Experimental Results

The hysteresis behavior of piezoelectric actuators including the residual displacement will be presented using the experimental results at different frequencies.

The hysteresis loop for piezoceramic actuator is defined at first quadrant because the input voltage is applied in the direction of polarization which causes an expansion [13]. The hysteresis loop in the piezoceramic actuator is asymmetric loop because of the mechanical bias that applied to the piezoactuator.

As the frequency of the input voltage increases the width of the hysteresis curve increases, the residual displacement increases, and the expansion of the piezoceramic decreases. It cannot reach more than 50% of the maximum piezoactuator expansion at 1 kHz.

The nominal input-output linear trajectory in (3.1) for 100 Hz:

$$y(t) = 1.6 + 0.26u(t) \quad (3.1)$$

where $y(t)$ is the piezoceramic displacement of the piezoceramic actuator (P-753.31C) and $u(t)$ input voltage. For 10 Hz the linear input-output is:

$$y(t) = 1.1 + 0.28u(t) \quad (3.2)$$

For 1 Hz the linear input-output is:

$$y(t) = 0.81 + 0.29u(t) \quad (3.3)$$

For 0.1Hz the linear input-output is:

$$y(t) = 0.58 + 0.30u(t) \quad (3.4)$$

Using the experimental results, nonlinearity in piezoceramic actuator at 70 sinusoidal voltages at different frequencies is shown in Table 3.1.

Table 3.1: Nonlinearity in piezoceramic actuator at 70 sinusoidal voltages at different frequencies

Frequency	0.1Hz	1Hz	10Hz	100Hz
Maximum nonlinearity	7.16%	7.45%	9.53%	18.44%
Average nonlinearity	2.91%	3.04%	3.54%	9.77%

We conclude that as the frequency of the input voltage increases the width of the hysteresis curve increases, the residual displacement increases, and the expansion of the piezoceramic decreases.

In Figure 3.8, piezoceramic displacement at 70 sinusoidal voltages at different frequencies are shown and nonlinearities in piezoceramic actuator are presented in Figure 3.9. When the input voltage (sinusoidal) is 70 volt at 10 Hz the maximum nonlinearity is 9.53% and residual displacement is 0.4899 μm . Similarly when the frequency 100 Hz the maximum nonlinearity is 18.44% and the residual displacement is 1.1164 μm .

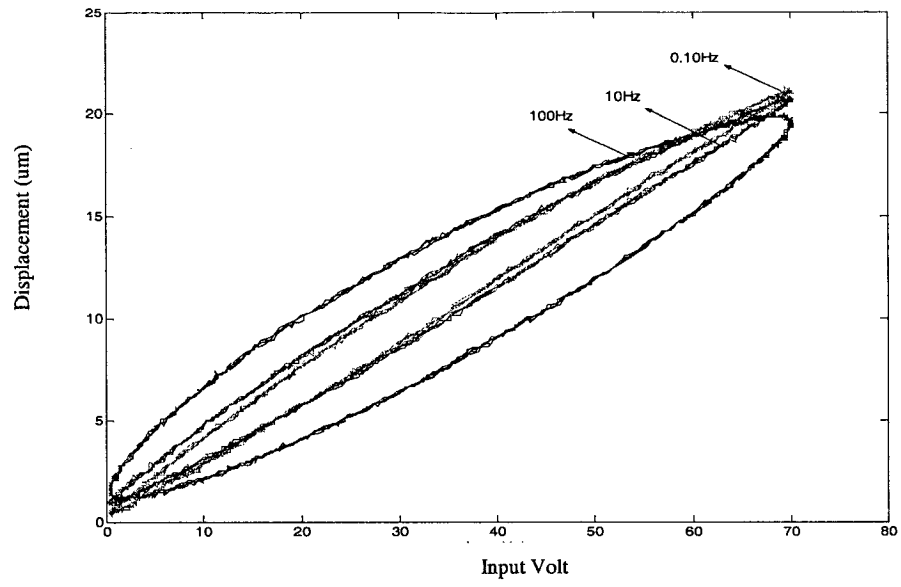


Figure 3.8: Hysteresis of piezoceramic actuator at different frequencies

Chapter 4

Hysteresis Modeling in Piezoceramic Actuator using Prandtl-Ishlinskii Model and Preisach Model

Modeling hysteresis in piezoceramic actuator will be presented using Prandtl-Ishlinskii Model and Preisach model. Parameters identification using experimental results will be presented.

4.1 Parameters Identification for Prandtl-Ishlinskii Model

The piezoceramic actuator response based on Prandtl-Ishlinskii is described in (4.1).

$$y(t) = \int_0^r p(r) E_r[v](t) dr \quad (4.1)$$

As mentioned in Section 2.4:

$$dr = r(i) - r(i-1) \quad (4.2)$$

$$y(t) = \sum_0^R p(r) E_r[v](t) (r(i) - r(i-1)) \quad (4.3)$$

$$p(r) = \alpha e^{-\beta(r-\delta)^2} \quad (4.4)$$

Prandtl-Ishlinskii operator (E):

$$E = \min(r, \max(-r, v)) \quad (4.5)$$

with

$$r = av + b \quad (5.6)$$

In Table 4.1, the parameters α , β , a , b , and δ were identified using the experimental data and nonlinear regression in MATHEMATICA 4.0.

Table 4.1: Identified parameters of the Prandtl-Ishlinskii model.

Frequency	Input volt	α	β	a	b	Density function	δ
0.1 Hz	0-40	5.79	0.000081	4.38	0.133	$p(r) = \alpha.e^{-\beta(r-\delta)^2}$	4
10Hz	0-70	5.65	0.000001	4.60	0.163	$p(r) = \alpha.e^{-\beta(r-\delta)^2}$	7
100Hz	0-70	5.16	0.000009	2.87	0.411	$p(r) = \alpha.e^{-\beta(r-\delta)^2}$	9.1

(1) Prandtl-Ishlinskii model for 40 sinusoidal input voltages at 0.10 Hz:

Measured and predicted piezoceramic displacement for 40 sinusoidal input voltages at 10 Hz is presented in Figure 4.1. The parameters α , β , a , b , and δ were identified using the experimental data and nonlinear regression in MATHEMATICA 4.0 (Table 4.1).

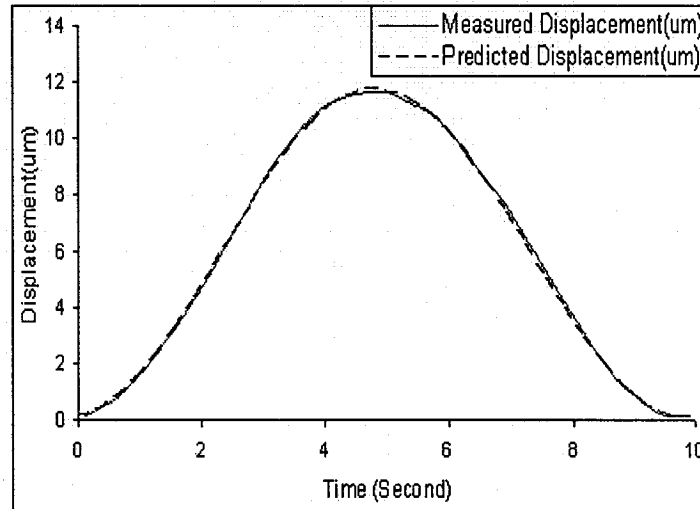


Figure 4.1: Measured and predicted displacement in piezoceramic actuator at 0.1 Hz sinusoidal voltage input (Prandtl-Ishlinskii model).

Measured and predicted hysteresis loop for 40 sinusoidal input voltages at 10 Hz using Prandtl-ishlinskii model is presented in Figure 4.1.

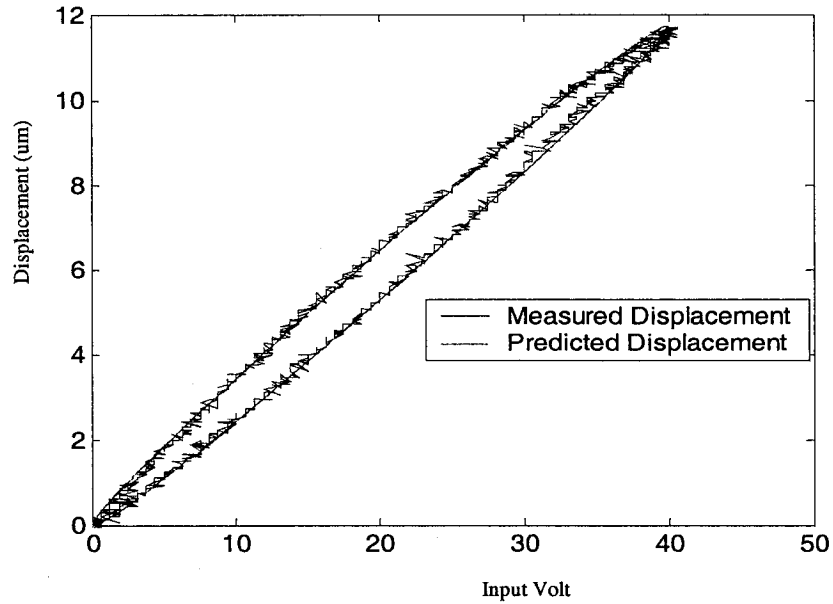


Figure 4.2: Measured and predicted hysteresis loop in piezoceramic actuator at 0.10 Hz sinusoidal voltage input (Prandtl-Ishlinskii Model)

Predicted error of piezoceramic displacement using Prandtl-ishlinskii model is shown in Figure 4.3. The average error is 0.841% whereas the maximum error is 4.730%.

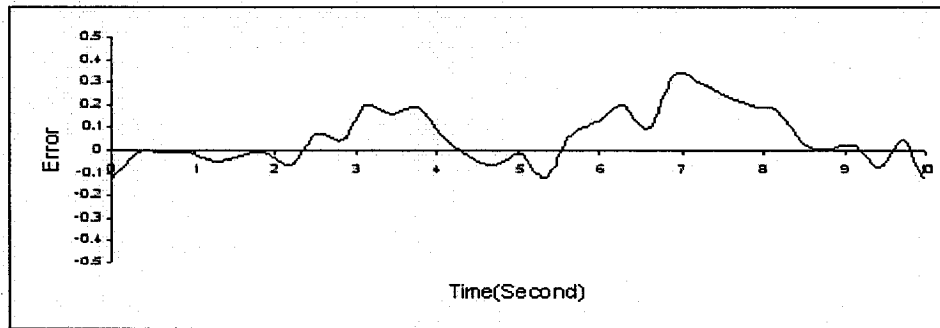


Figure 4.3: Predicted error of displacement in piezoceramic actuator at 0.10 Hz sinusoidal voltage input (Prandtl-Ishlinskii model).

(2) Prandtl-Ishlinskii model for 70 sinusoidal input voltage 10 Hz:

Measured and predicted piezoceramic displacement response for 70 sinusoidal input voltages at 10 Hz is presented in Figure 4.4. The parameters α , β , a , b , and δ were identified using the experimental data and nonlinear regression in MATHEMATICA 4.0 (Table 4.1).

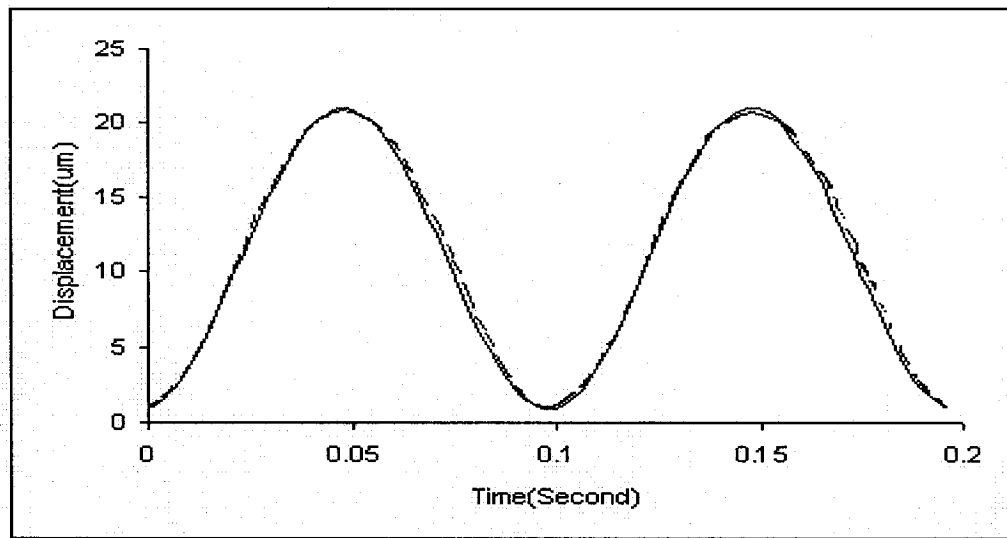


Figure 4.4: Measured and predicted displacement in piezoceramic actuator at 10 Hz sinusoidal voltage input (Prandtl-Ishlinskii model).

Measured and predicted hysteresis loop for 70 sinusoidal input voltages at 10 Hz using Prandtl-Ishlinskii model is presented in Figure 4.5.

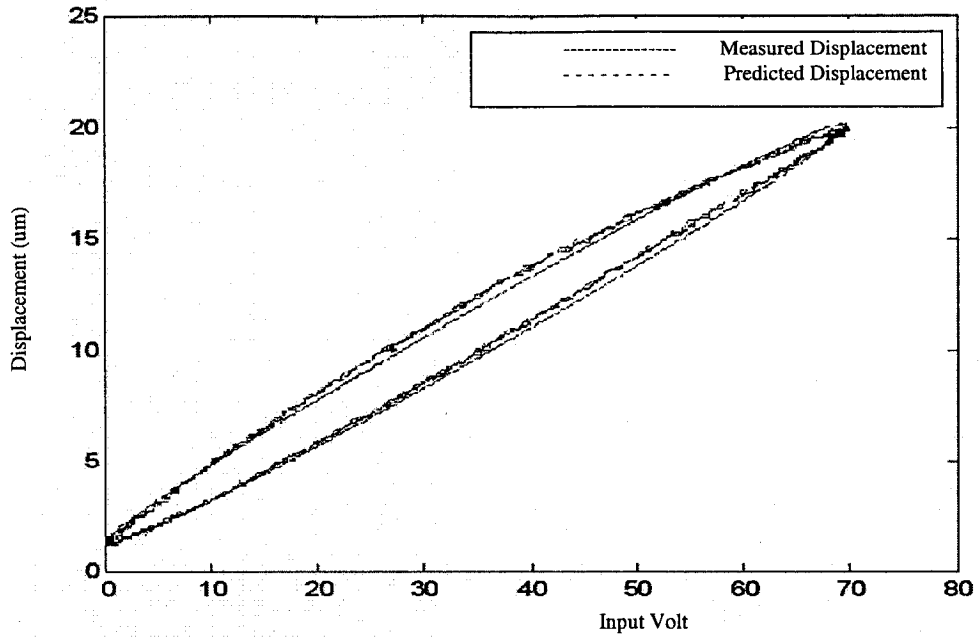


Figure 4.5: Measured and predicted hysteresis loop in piezoceramic actuator at 10 Hz sinusoidal voltage input (Prandtl-Ishlinskii Model).

Predicted error of piezoceramic displacement using Prandtl-ishlinskii model is shown in Figure 4.6. The average error is 1.302% whereas the maximum error is 4.406%.

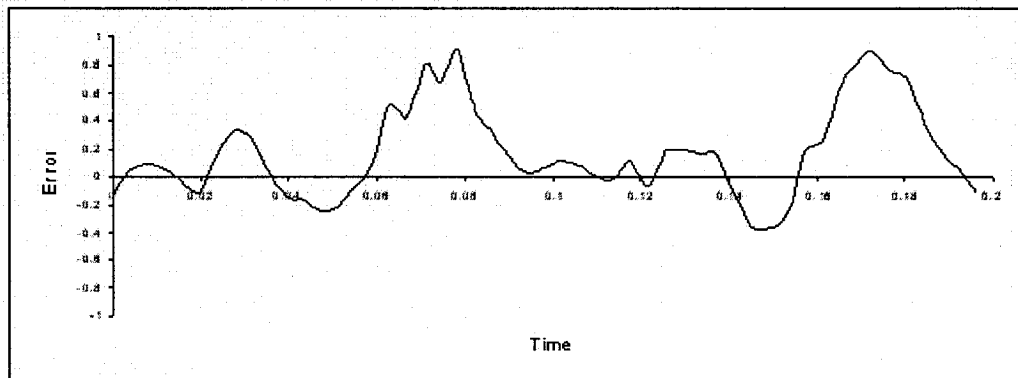


Figure 4.6: Predicted error of displacement in piezoceramic actuator at 10 Hz sinusoidal voltage input (Prandtl-Ishlinskii model).

(3) Prandtl-Ishlinskii model for 70 sinusoidal input voltages at 100 Hz:

Measured and predicted piezoceramic displacement for 70 sinusoidal input voltages at 100 Hz using Prandtl-Ishlinskii model is presented in Figure 4.8. The parameters α , β , a , b , and δ were identified using the experimental data and nonlinear regression in MATHEMATICA 4.0 (Table 4.1).

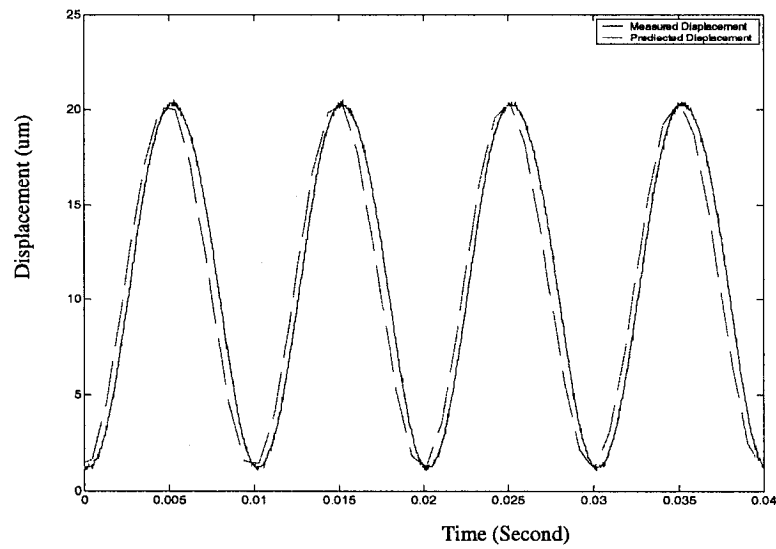


Figure 4.7: Measured and predicted displacement in piezoceramic actuator at 100 Hz sinusoidal voltage input (Prandtl-Ishlinskii model).

Measured and predicted hysteresis loop for 70 sinusoidal input voltages at 10 Hz using Prandtl-ishlinskii model is presented in Figure 4.9.

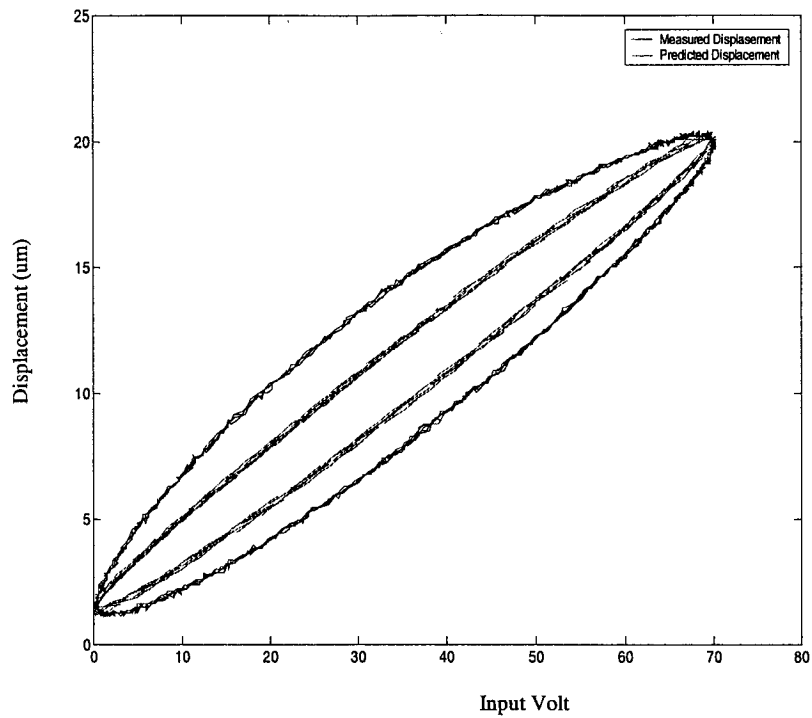


Figure 4.8: Measured and predicted hysteresis loop in piezoceramic actuator at 100 Hz sinusoidal voltage input (Prandtl-Ishlinskii Model).

Predicted error of piezoceramic displacement using Prandtl-ishlinskii model is shown in Figure 4.9. The average error is 10.26% whereas the maximum error is 21.6%.

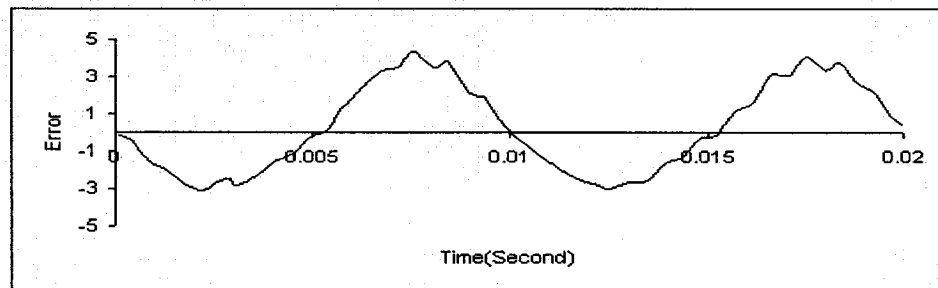


Figure 4.9 Predicted error of displacement in piezoceramic actuator at 100 Hz sinusoidal voltage input (Prandtl-Ishlinskii model).

4.2 Parameters Identification for Preisach Model

In (4.7) and (4.8) give a numerical form of the Preisach model that can be formed to calculate the piezoelectric response [31].

$$\dot{u}(t) < 0, x(t) = \sum_{k=1}^{n-1} [X(\alpha_k, \beta_{k-1}) - X(\alpha_k, \beta_k)] + [X(\alpha_n, \beta_{n-1}) - X(\alpha_n, u(t))] \quad (4.7)$$

$$\dot{u}(t) > 0, x(t) = \sum_{k=1}^{n-1} [X(\alpha_k, \beta_{k-1}) - X(\alpha_k, \beta_k)] + X(u(t), \beta_{n-1}) \quad (4.8)$$

In order to implement the two equations a series of functions $f_{\alpha\beta}$ and f_{β} for the specific piezoceramic actuator that being used need to be experimentally determined for all the points [31, 13, 14].

The Preisach function when $\alpha = \beta$ is:

$$f_{\beta} = a_0 + a_1 \cdot \alpha + a_2 \cdot \beta \quad (4.10)$$

and the Preisach function, when $\alpha \neq \beta$ is:

$$f_{\alpha\beta} = b_0 + b_1 \cdot \alpha + b_2 \cdot \beta + b_3 \cdot \alpha \cdot \beta \quad (4.11)$$

The constants in (4.10) and (4.11) were identified via the experimental results using the least square method in MATLAB 6.5 and MATHEMATICA 4.0 .

(1) Preisach model for 70 sinusoidal input at 10 Hz:

Measured and predicted piezoceramic displacement for 40 sinusoidal input voltages at 0.10 Hz using Preisach model is presented in Figure 4.8. The constants for the Preisach model in (4.7-4.14) were identified via the experimental results using the least square method in MATLAB 6.5 and MATHEMATICA 4.0.

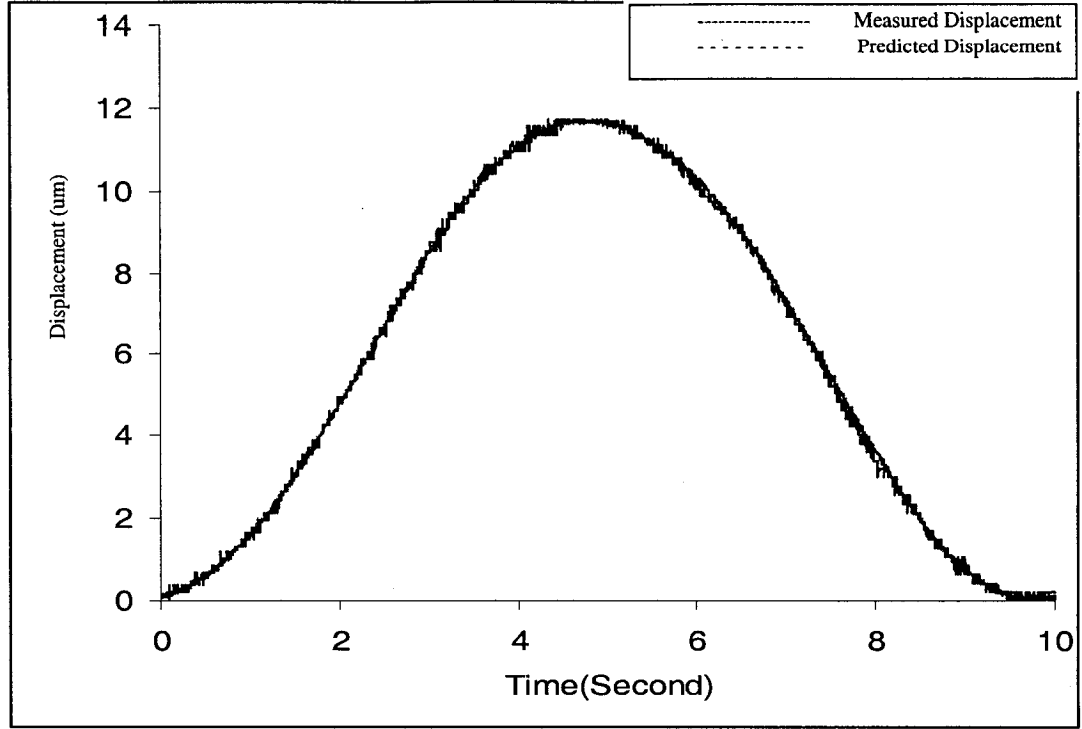


Figure 4.10: Measured and predicted displacement in piezoceramic actuator at 0.1 Hz sinusoidal voltage input (Preisach model).

a) For $\dot{u} > 0$:

$$f_{0-10} = -0.08410 + 0.12595.\alpha + 0.12595.\beta \quad (4.7)$$

$$f_{10-20} = -0.35910 + 0.14185.\alpha + 0.14185.\beta \quad (4.8)$$

$$f_{20-30} = -0.72440 + 0.15115.\alpha + 0.15115.\beta \quad (4.9)$$

$$f_{30-40} = -0.46520 + 0.15002.\alpha + 0.15002.\beta \quad (4.10)$$

b) For $\dot{u} < 0$:

$$f_{40-30} = 0.00145514 + 0.00014726.\alpha + 0.05820544.\beta + 0.00589042.\alpha.\beta \quad (4.11)$$

$$f_{30-20} = 0.00071830 + 0.00016889.\alpha + 0.02873216.\beta + 0.00675578.\alpha.\beta \quad (4.12)$$

$$f_{20-10} = 0.00030484 + 0.00018962.\alpha + 0.01219315.\beta + 0.00758485.\alpha.\beta \quad (4.13)$$

$$f_{10-0} = 0.02001000 - 0.00037489.\alpha + 0.00850468.\beta + 0.00850468.\alpha.\beta \quad (4.14)$$

Measured and predicted hysteresis loop for 40 sinusoidal input voltages at 0.10 Hz using Preisach model is presented in Figures 4.9 and 4.10.

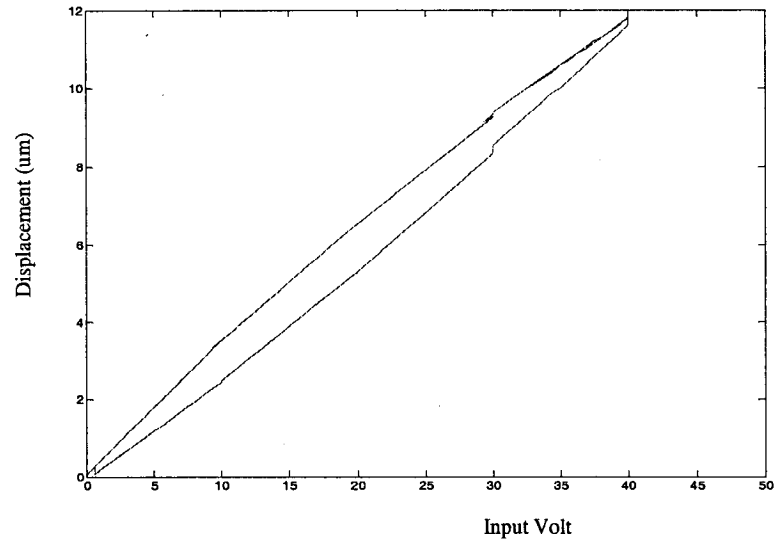


Figure 4.11: Predicted hysteresis loop in piezoceramic actuator at 0.10 Hz sinusoidal voltage input (Preisach Model)

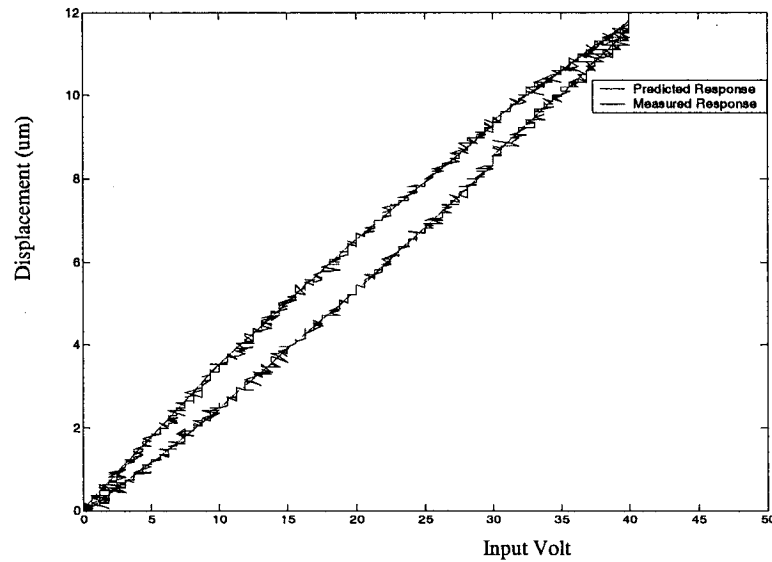


Figure 4.12 Measured and predicted hysteresis loop in piezoceramic actuator at 0.10 Hz sinusoidal voltage input (Preisach Model).

Predicted error of piezoceramic displacement using Preisach model is shown in Figure 4.11. The average error is 0.864% whereas the maximum error is 4.712%.

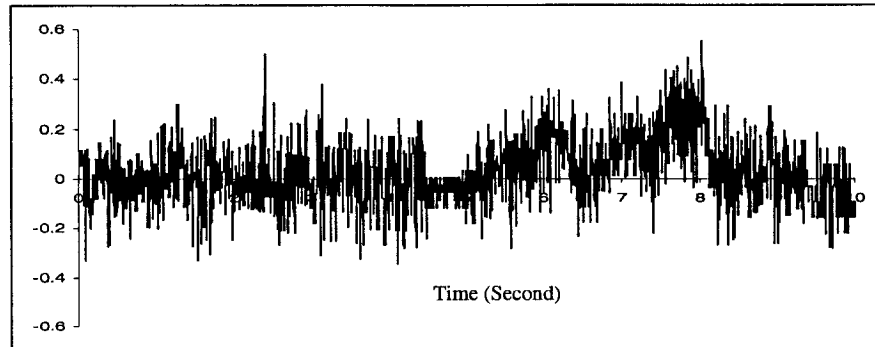


Figure 4.13: Predicted error of displacement in piezoceramic actuator 0.10 Hz sinusoidal input voltage (Preisach Model)

(2) Preisach model for 70 sinusoidal input at 10 Hz:

Measured and predicted piezoceramic displacement for 70 sinusoidal input voltages at 10 Hz using Preisach model is presented in Figure 4.15. The constants for the Preisach model in (4.15-4.28) were identified via the experimental results using the least square method in MATLAB 6.5 and MATHEMATICA 4.0.

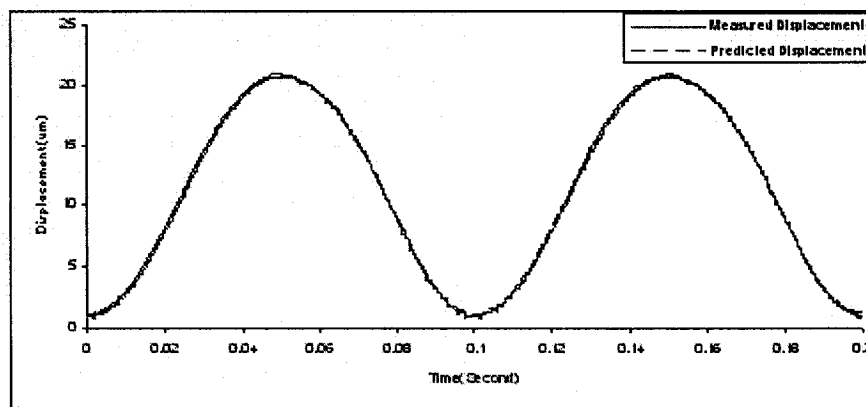


Figure 4.14: Measured and predicted displacement in piezoceramic actuator at 10 Hz sinusoidal voltage input (Preisach model).

a) For $\dot{u} > 0$:

$$f_{00-10} = 0.7599 + 0.1128.\alpha + 0.1128.\beta \quad (4.15)$$

$$f_{10-20} = 0.2681 + 0.1379.\alpha + 0.1379.\beta \quad (4.16)$$

$$f_{20-30} = 0.1229 + 0.1411.\alpha + 0.1411.\beta \quad (4.17)$$

$$f_{30-40} = -0.6658 + 0.1529.\alpha + 0.1529.\beta \quad (4.18)$$

$$f_{40-50} = -0.9984 + 0.1507.\alpha + 0.1507.\beta \quad (4.19)$$

$$f_{50-60} = 0.0066 + 0.1471.\alpha + 0.1471.\beta \quad (4.20)$$

$$f_{60-70} = -1.1665 + 0.1506.\alpha + 0.1506.\beta \quad (4.21)$$

b) For $\dot{u} < 0$:

$$f_{70-60} = 0.00148696 + 0.63997799.\alpha + 0.1040869.\beta - 0.00638949.\alpha.\beta \quad (4.22)$$

$$f_{60-50} = 0.00148696 + 0.63997799.\alpha + 0.1040869.\beta - 0.00638949.\alpha.\beta \quad (4.23)$$

$$f_{50-40} = 0.00090754 + 0.00004963.\alpha + 0.06352769.\beta - 0.00347407.\alpha.\beta \quad (4.24)$$

$$f_{40-30} = 0.000453521 + 4.4916100.\alpha + 0.03174619.\beta - 0.00427159.\alpha.\beta \quad (4.25)$$

$$f_{30-20} = 0.000451726 + .000060229.\alpha + 0.03162079.\beta - 0.00427159.\alpha.\beta \quad (4.26)$$

$$f_{20-10} = 0.000451726 + .0000610229.\alpha + 0.03162079.\beta - 0.00427159.\alpha.\beta \quad (4.27)$$

$$f_{10-0} = 0.00020891 + .0000740558.\alpha + 0.01462339.\beta - 0.00518391.\alpha.\beta \quad (4.28)$$

Measured and predicted hysteresis loop for 70 sinusoidal input voltages at 10 Hz using Preisach model is presented in Figure 4.16.

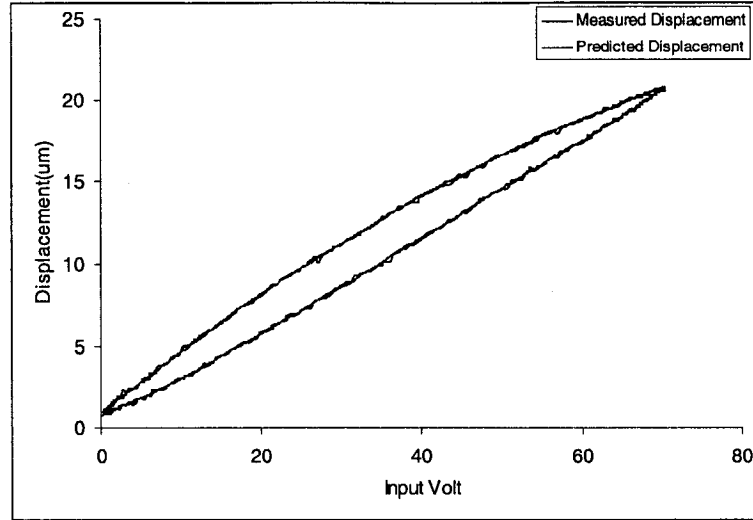


Figure 4.15: Measured and predicted hysteresis loop in piezoceramic actuator at 10 Hz sinusoidal voltage input (Preisach model).

Predicted error of piezoceramic displacement using Preisach model is shown in Figure 4.17. The average error is 0.3782% whereas the maximum error is 1.843%.

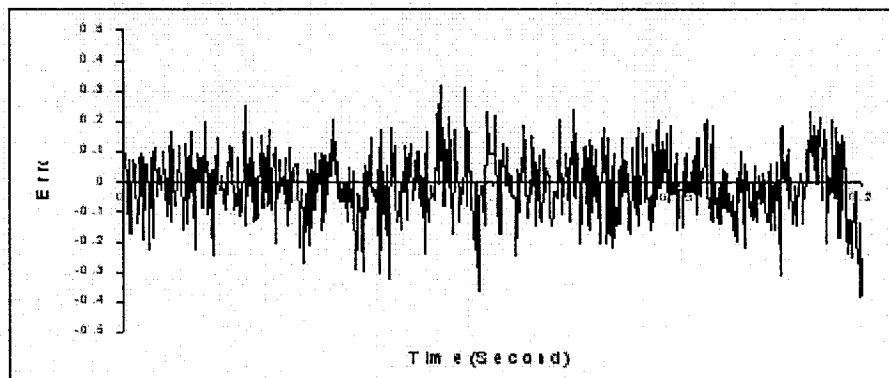


Figure 4.16: Predicted error of displacement in piezoceramic actuator at 10 Hz sinusoidal voltage input (Preisach Model).

(3) Preisach model for 70 sinusoidal input at 100 Hz:

Measured and predicted piezoceramic displacement for 70 sinusoidal input voltages at 100 Hz using Preisach model is presented in Figure 4.18. The constants

for the Preisach model in (4.29-4.45) were identified via the experimental results using the least square method in MATLAB 6.5 and MATHEMATICA 4.0.

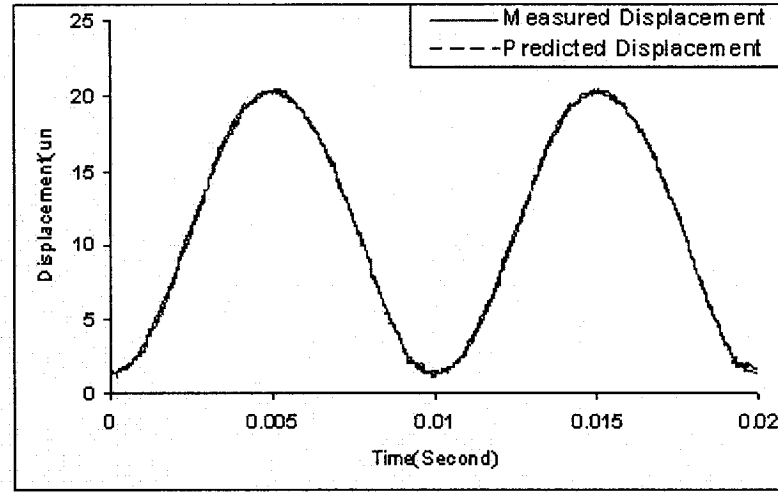


Figure 4.17 Measured and predicted displacement in piezoceramic actuator at 100 Hz sinusoidal voltage input (Preisach model).

a) For $\dot{u} > 0$:

$$f_{0-10} = 1.1388 + 0.0410.\alpha + 0.0410.\beta \quad (4.29)$$

$$f_{10-20} = -0.0213 + 0.1053.\alpha + 0.1053.\beta \quad (4.30)$$

$$f_{20-30} = -0.4615 + 0.1178.\alpha + 0.1178.\beta \quad (4.31)$$

$$f_{30-40} = -1.6700 + 0.1361.\alpha + 0.1361.\beta \quad (4.32)$$

$$f_{40-50} = -2.2186 + 0.1434.\alpha + 0.1434.\beta \quad (4.33)$$

$$f_{50-60} = -4.6638 + 0.1677.\alpha + 0.1677.\beta \quad (4.34)$$

$$f_{60-70} = -9.8851 + 0.2099.\alpha + 0.2099.\beta \quad (4.35)$$

b) For $\dot{u} < 0$:

$$f_{70-67.5} = 0.00506099 - .0000137822.\alpha + 0.35426901.\beta - 0.000964756.\alpha.\beta \quad (4.36)$$

$$f_{67.5-62.5} = 0.00445621 - 0.000005143.\alpha + 0.31193410.\beta - 0.00035948.\alpha.\beta \quad (5.37)$$

$$f_{62.5-60} = 0.002081731 - 0.00003114.\alpha + 0.145721005.\beta - 0.00218004.\alpha.\beta \quad (4.38)$$

$$f_{60-50} = 0.00194023 - 0.0000336083.\alpha + 0.13581599.\beta - 0.002352589.\alpha.\beta \quad (4.39)$$

$$f_{50-40} = 0.00145558 - 0.0000433148.\alpha + 0.10189099.\beta - 0.003032031.\alpha.\beta \quad (4.40)$$

$$f_{40-30} = 0.00127771 - 0.0000474491.\alpha + 0.08943895.\beta - 0.003321473.\alpha.\beta \quad (4.41)$$

$$f_{30-20} = 0.000817715 - 0.0000627277.\alpha + 0.05723995.\beta - 0.00439094.\alpha.\beta \quad (4.42)$$

$$f_{20-10} = 0.06693863 + 0.6627056771.\alpha + 0.04631519.\beta - 0.004415833.\alpha.\beta \quad (4.43)$$

$$f_{10-2.5} = 1.013929088 + 0.9476639.\alpha + 0.0195378524.\beta - 0.0072809088.\alpha.\beta \quad (4.44)$$

$$f_{2.5-0} = 0.000285383 + 0.000164049.\alpha + 0.019976811.\beta - 0.01148337.\alpha.\beta \quad (4.45)$$

Measured and predicted hysteresis loop for 70 sinusoidal input voltages at 10 Hz using Preisach model is presented in Figure 4.18.

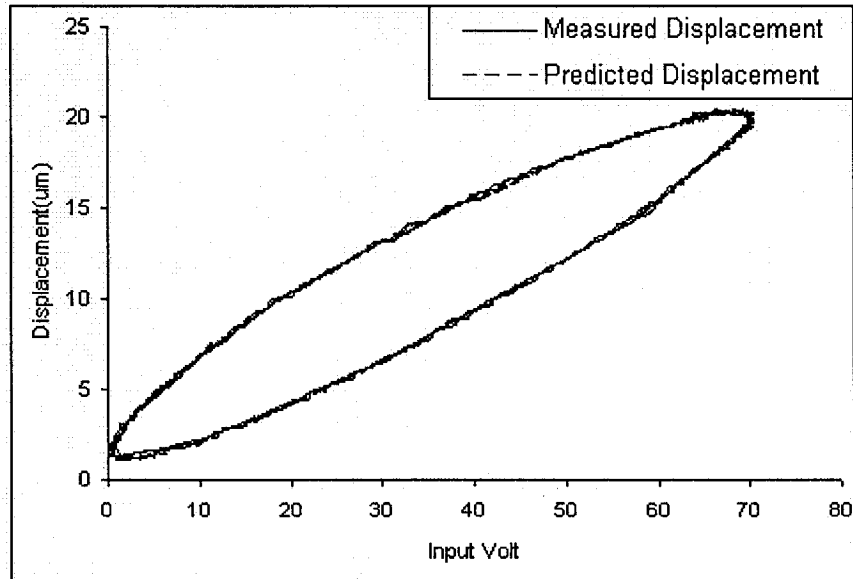


Figure 4.18: Measured and predicted hysteresis loop in piezoceramic actuator at 100 Hz sinusoidal voltage input (Preisach model).

Predicted error of piezoceramic displacement is shown in Figure 4.19. The average error is 2.981% whereas the maximum error is 0.591%.

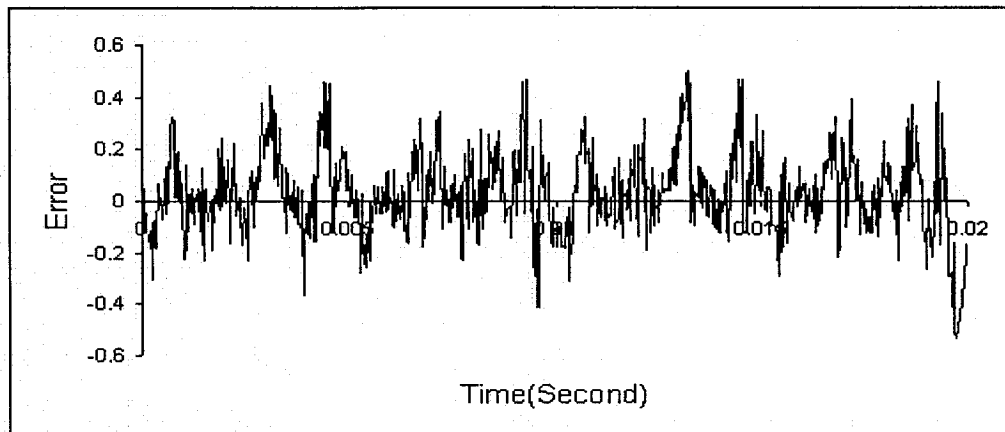


Figure 4.19: Predicted error of displacement in piezoceramic actuator at 100 Hz sinusoidal voltage input (Preisach model).

5.3 Comparison between Preisach model and Prandtl-Ishlinskii model

Prandtl-Ishlinskii model has some very unique properties that is invertible and the inversion has the same structure [36, 18]. But for the Preisach model it is not possible to drive a function for the inverse analytically [26]. In Table 4.2, comparison between the Preisach model and Prandtl-Ishlinskii model is presented. When the input voltage (sinusoidal) is 70 volt, at 10 Hz the maximum predicted error using Preisach model is 1.84% whereas the maximum predicted error using Prandtl-Ishlinskii model is 4.41%.

Prandtl-Ishlinskii model may suitable to describe the displacement in piezoactuator while Preisach model is more accurate but the displacement signal arising a lot of complications in simulation and being time consuming.

Table 5.2: Error of predicted (Prandtl-Ishlinskii and Preisach) displacement in piezoceramic actuator at different frequencies.

Frequency	Input volt	Maximum error[PI]	Average error [PI]	Maximum error [P]	Average error [P]
0.1Hz	[0-40]	4.92%	0.89%	4.71%	0.86%
10Hz	[0-70]	4.40%	1.30%	1.84%	0.38%
100Hz	[0-70]	21.60%	10.26%	2.61%	0.57%

Chapter 5

Conclusion and Future Work

5.1 Conclusion

In this work, hysteresis in piezoceramic actuator was studied. As the frequency of the input voltage increases, the width of the hysteresis curve increases and the residual displacement also increases. When the input voltage (sinusoidal) is 70 volt at 10 Hz the maximum nonlinearity is 9.53% and residual displacement is 0.4899 μm . Similarly when the frequency 100 Hz the maximum nonlinearity is 18.44% and the residual displacement is 1.1164 μm , which clear shows the effects of hysteresis need to be considered.

Preisach model and Prandtl-Ishlinskii model for hysteresis in the piezoceramic actuator have been implemented. Experimental data shows that when the input voltage (sinusoidal) is 70 volt, at 10 Hz the maximum predicted error using Preisach model is 1.84% whereas the maximum predicted error using Prandtl-Ishlinskii model is 4.41%. Prandtl-Ishlinskii model may suitable to describe the displacement in piezoactuator while Preisach model is more accurate but the displacement signal arising a lot of complications in simulation and being time consuming .

5.2 Future Work:

To make the research more appreciated three recommendations can be made:

- (1) Identify dynamic parameter for the Prandtl-Ishlinskii operator. Subsequently new approach will be developed to describe rate dependent case.
- (2) Develop a control framework for piezoceramic actuator to reduce hysteresis effects with ensure stability of the system.
- (3) Design compensator to generate an inverse feedforward controller for the piezoceramic actuator by using the inversion property in Prandtl-Ishlinskii model.

References

- [1] P. A. Mackeyville, *Piezoceramics Actuator: Principles and Applications*, APC International, Ltd, 2002.
- [2] B. Zhang and Z. Zhu, Developing a linear piezomotor with nanometer resolution and high stiffness, *IEEE/ASME Trans. Mechatronics* , Vol.2, 1997, 22–29.
- [3] J. D. Kim and S. R. Nam , Development of a micro-depth control system for an ultra-precision lathe using a piezo-electric actuator, *International Journal of Machine Tools and Manufacture*, Vol. 37, Issue 4, 1997, 495-509.
- [4] Jaechun, Ryu, and Chongkug, Force control of a flexible robotic finger with Piezoelectric actuators using fuzzy algorithms, *SICE*, 26-28, 1995, 26-28.
- [5] M. Sasaki, T. Suzuki, E. Ida, F. Fujisawa, M. Kobayashi and H. Hiria, Track-following control of a dual-stage hard disk drive using a neuro-control system. *Eng. Appl. Artif. Intell.* Vol.11, 1998, 707–716.
- [6] B. N. Agrawal, M. A. Elshafei and G. Song, Adaptive antenna shape control using piezoelectric actuators. *Acta Astronaut.* Vol. 40, 1997, 821–826.
- [7] J. H. Park, K. Yoshida and S. Yokoto, Resonantly driven piezoelectric micropump – fabrication of a micropump having high power density, *Mechatronics*, Vol. 9, 1999, 687–702.

- [8] W. H. Zhu, B. J. Martin, and Y. Altintas, A fast tool servo design for precision turning of shafts on conventional CNC lathes, *International Journal of Machine Tools and Manufacture*, Vol. 41, Issue 7, 2001, 953-965.
- [9] S. B. Choi, H. K. Kim, S. C. Lim and Y. P. Park, Position tracking control of an optical pick-up device using piezoceramic actuator, *Mechatronics*, Vol. 11, Issue 6, 2001, 691-705.
- [10] R. B. Mrad and H. Hu, A model for voltage-to-displacement dynamics in piezoceramic actuators subject to dynamic voltage excitations. *IEEE/ASME Transactions on Mechatronics*, Vol. 74, 2002, 479-489.
- [11] J. Kim and S. Nam. Development of a micro-positioning grinding table using piezoelectric voltage feedback. In: *Proceeding of the Institution of Mechanical Engineers Part B—Journal of Engineering Manufacture*, Vol. 209, 1995, 469-474.
- [12] S. B. Jung and S. W. Kim, Improvement of scanning accuracy of PZT piezoelectric actuator by feed-forward model-reference control, *Precision Engineering*, 1994, Vol.16, 49-55.
- [13] P. Ge and M. Jouaneh, Modeling hysteresis in Piezoceramics, *Precision Engineering*, Vol. 17, 1995, 211-221.
- [14] P. Ge and M. Jouaneh, Generalized Preisach model for hysteresis nonlinearity of Piezoceramic actuators, *Precision Engineering*, Vol. 20, Issue 2, 1997, 99-111.
- [15] D. Hughes and J. T. Wen, Preisach modeling of Piezoceramic and shape memory alloy hysteresis. *SPIE Proceeding 2715*, 1995, 507-528.
- [16] D. Hughes and J. T. Wen, Preisach modeling of Piezoceramic and shape memory alloy hysteresis, *Smart Materials and Structures*, Vol. 6, 1997, 287-300.

- [17] Y. Stepanenko and C.Y. Su, Intelligent Control of Piezoelectric Actuators, IEEE Conference on Decision & Control, 37th IEEE, Temapa, 4234-4239 1998.
- [18] K. Kuhnen and H. Janocha, Real-time Compensation of Hysteresis and Creep in Piezoelectric Actuators, Sensors and Actuators, Vol.79, 2000, 83-89.
- [19] W. T. Ang, F. A. Garmon, P.K. Khosla, and C.N. Riviere, Modeling rate-dependent hysteresis in piezoelectric actuators, IEEE, Int. Conference on Intelligent Robots and Systems, Vol. 2, 2003, 1975-1980.
- [20] J. J. Tzen, S. L. Jeng, and W.H. Chieng, Modeling of piezoelectric actuator for compensation and controller design, Precision Engineering, Vol. 27, 2003, 70-86.
- [21] D. Song and J. Li, Modeling of piezo actuator's nonlinear and frequency dependent dynamic, Mechatronics, Vol. 9, 1999, 391-410.
- [22] Physik Instrumente Company, Operating Manual, 2001.
- [23] J. W. Macki, P. Nister, and P. Zecca, Mathematical Models of Hysteresis, SAIM REVIEW, Vol.35, No. 1, 394-123, 1993.
- [24] F. Z. Preisach, On magnetic Aftereffect, Vol.94, 1935, 94-277.
- [25] M. L. Hondong, Mathematical theory and calculations of magnetic hysteresis curves, IEEE Transactions on control systems technology, Vol. 24, 1988, 3120-3122.
- [26] W. Galinaities, Two methods for modeling scalar hysteresis and their using in controlling actuators with hysteresis, PhD thesis, Blacksburg, Virginia, USA, 1999.
- [27] J. D. Kim and S. R. Nam. Development of a micro-positioning grinding table using piezoelectric voltage feedback, Precision Engineering, 209, 1995.

- [28] G. Salvady, P. N. Sreeram, G. Naganathan, Hysteresis model for piezoceramic actuator systems using Preisach models, in: Proceedings of the North American Conference on Smart Structures and Materials, Orlando, Florida, 13–18, 1994.
- [29] P. N. Sreeram and N. G. Naganathan, Hysteresis prediction for a piezoceramic material system. In: Proceeding of 1993 ASME Winter Annual Meeting, New Orleans, LA Vol. AD-Vol33, 1993, 35–42.
- [30] J. Manuel, C. Hernandez and V. Hayward, Phase control approach to hysteresis reduction, IEEE Transactions on control systems technology, Vol. 9, Issue 1, 2001, 17-26.
- [30] X. Tan and J. S. Baras, A Robust Control Framework for Smart Actuator, IEEE American Control Conference, Vol. 6, 2003, 4645-4650.
- [31] I. D. Mayergoyz, Mathematical Models of Hysteresis, Springer, New York, NY, 2003.
- [32] Y. Yu, N. Naganathan, and R. Dukkipati, Preisach Modeling of Hysteresis for Piezoactuator System, Mechanism and Machine Theory, Vol. 37, 2002, 49-59.
- [33] I. Mayergoyz, Hysteresis from the mathematical and control theory points of view, Journal of Applied Physics, Vol. 57, 1985, 3803-3805.
- [34] D.A. Hall, Nonlinearity in Piezoelectric Ceramics, Journal of Materials Science 36, 4575-4601, 2001.
- [35] F. Vestroni and M. Noori, Hysteresis in mechanical systems-modeling and dynamic response, International Journal of Nonlinear Mechanics, Vol. 37, 1261-1262, 2002.

- [36] Q. Wang and C.Y. Su, Robust Adaptive Control of A Class of Nonlinear Systems Including Actuator Hysteresis with Prandtl-Ishlinskii Presentation, Submitted to "Automatica", Jan 2004.
- [37] M. Brokate and J. Sprekels, Hysteresis and Phase Transitions, Springer New York, 1996.
- [38] B. M. Chen, T. H. Lee, C.C. Hang, Y. Guo, and S. Weerasooriya, An Almost Disturbance Decoupling Robust Controller Design for a Piezoelectric Bimorph Actuator with Hysteresis, IEEE Tran. Automation and Control, Vol. 7, No. 2, 160-174, 1999.
- [39] H. Hu, R. Ben Mrad, A discrete-time compensation algorithm for hysteresis in piezoceramic actuators, Mechanical systems and signal processing, vol.18, 169-185, 2004.
- [40] L. Prandtl, Ein gedankenmodell zur kinenschen thorie festen Korper, ZAMM, vol. 8, 85-106, 1928.
- [41] G. Tao and P.V. Kokotovic, adaptive control of plants with unknown hysteresis, IEEE Trans. On Automatic Control, Vol. 40,200-212, 1995.